

Storm Surge Computations for the North Carolina Sea Level Rise Risk Management Study

A RENCI Technical Report
TR-12-04

Brian Blanton, PhD

Renaissance Computing Institute (RENCI)
University of North Carolina at Chapel Hill
blanton@renci.org

Prepared for:

North Carolina Division of Emergency
Management, Office of Geospatial and
Technology Management

renci

www.renci.org

Prepared for:

**NORTH CAROLINA DIVISION OF EMERGENCY MANAGEMENT
OFFICE OF GEOSPATIAL AND TECHNOLOGY MANAGEMENT**



Storm Surge Computations for the North Carolina Sea Level Rise Risk Management Study

Prepared by

Brian Blanton, Ph.D.

Renaissance Computing Institute

University of North Carolina at Chapel Hill

November 12, 2012

Version 1.0

CONTENTS

Contents	2
1. Overview of ADCIRC Application	3
1.1. The Use of ADCIRC to Evaluate the Coastal Flooding Hazard for the North Carolina Sea Level Rise Risk Management Study.....	3
1.2. Review of Methodology for the North Carolina Flood Insurance Study.....	3
2. ADCIRC-related TASKS	4
2.1. Task 1: Support JPM Sensitivity Test.....	4
2.2. Task 2: Wind Field Generation	6
2.3. Task 3: Tidal Datum Code	6
2.4. Task 4: Perform Baseline Simulations	6
2.4.1 <i>Equilibrium tidal solution</i>	6
2.4.2 <i>Tidal Datums</i>	6
2.4.3 <i>Simulation of Historical Hurricanes</i>	8
2.4.4 <i>Production storm surge simulations</i>	9
2.4.5 <i>Statistical synthesis</i>	11
2.5. Task 5: Perform Sea Level Rise Scenario Simulations	12
2.5.1 <i>20 cm Scenario</i> :.....	13
2.5.2 <i>40 cm Scenario</i> :.....	14
2.5.3 <i>60 cm Scenario</i> :.....	15
2.5.4 <i>80 cm Scenario</i> :.....	16
2.5.5 <i>100 cm Scenario</i> :.....	17
2.6. Task 6: Storminess statistical analyses.....	18
2.6.1: <i>20 cm SLR and Mid 21st Century</i> :.....	19
2.6.2: <i>40 cm SLR and Mid 21st Century</i> :.....	20
2.6.3: <i>40 cm SLR and End 21st Century</i> :.....	21
2.6.4: <i>60 cm SLR and Mid 21st Century</i> :.....	22
2.6.5: <i>60 cm SLR and End 21st Century</i> :.....	23
2.6.6: <i>80 cm SLR and Mid 21st Century</i> :.....	24
2.6.7: <i>80 cm SLR and End 21st Century</i> :.....	25
2.6.8: <i>100 cm SLR and Mid 21st Century</i> :.....	26
2.6.9: <i>100 cm SLR and End 21st Century</i> :.....	27
2.7. Overview of statistical results	28
3. Cape Fear water levels	30
3.1. Idealized Model Experiments	31
3.2. Idealized Model Results	34
3.3. Connection of Idealized Results to NC-SLRIS	36
3.4. Idealized Results Conclusion	40
4. References	41

1. OVERVIEW OF ADCIRC APPLICATION

1.1. The Use of ADCIRC to Evaluate the Coastal Flooding Hazard for the North Carolina Sea Level Rise Risk Management Study

To address the evaluation of the coastal hazard component for the North Carolina Sea Level Rise Impacts Study (NC-SLRIS), the Renaissance Computing Institute (RENCI) proposed an approach that follows conceptually the application of the tidal and storm surge model ADCIRC for computing flood hazard levels for the recent Flood Insurance Study (FIS) for North Carolina's coastal counties. The FIS approach uses a high-resolution numerical model grid for storm surge and waves based on recent topographic surveys and best-available bathymetric data, as well as advanced statistical techniques for modeling North Carolina's tropical storm climate. The approach addresses conduction and management of needed simulations on RENCI's high-performance computers.

1.2. Review of Methodology for the North Carolina Flood Insurance Study

RENCI recently computed flood hazard data for the North Carolina Floodplain Mapping Program (NCFMP) Flood Insurance Study (FIS) for coastal counties. The computational system (Blanton, 2008) developed for the FIS uses state-of-the-art numerical models, including the storm surge and tidal model ADCIRC (Westerink et al, 2008), and uses computer resources at RENCI for the actual computations. This system has been tested several times in the past three years, and RENCI considers this system acceptably robust for the purposes of NC-SLRIS.

The NC FIS project developed a comprehensive digital elevation model (DEM) using recent coastal LIDAR data as well as best-available bathymetric data. This DEM was used to develop the ADCIRC grid that is being used for the flood hazard simulations. Additionally, the Joint Probabilities Method (JPM) approach to model the current tropical storm population (P. Vickery, Applied Research Associates) represented an advanced application of JPM to substantially reduce the numerical model computational resource requirements.

In the NC FIS system, the parametric boundary layer model HBL (Vickery et al, 2009) models the tropical storm wind and pressure fields. Storm parameters for HBL are derived through the above-mentioned JPM approach. The extratropical component is modeled with analyzed wind and pressure fields from OceanWeather, Inc.

In the NC SLR RMS context, the primary components of the NC FIS will be used. This includes the model ADCIRC, a comprehensive ADCIRC grid for the region, and a modification of the storm tracks developed for the FIS, considered the baseline storm population for SLR RMS. These storms, and modifications that represent future storm climates, are described elsewhere in the Task 2 approach (ARA, Peter Vickery). The existing extratropical storm set for the FIS will be used for any required extratropical simulations.

2. ADCIRC-RELATED TASKS

The RENCI/UNC scope consists of 6 tasks, numbered the same as in the RFDO. Task 3 (Tidal Datum Code) was not part of the final RENCI project; however, we retain the same numbering as in the RFDO for clarity. The specific tasks are as follows, each of which is detailed in the subsequent sections of the report.

Task 1: Support JPM Sensitivity Tests with ARA

Task 2: Wind Field Generation

Task 3: Tidal Datum Code

Task 4: Perform Baseline Simulations – present-day ADCIRC grid and storm climate

Task 5: Perform Future SLR/Geomorphological Simulations – ADCIRC grids and/or increased mean sea level that correspond to 20 cm, 40 cm, 60 cm, 80 cm, and 100 cm scenarios.

Task 6: Storminess Incorporation

Tasks 1, 2, and 6 are to compute specific analyses and/or inputs to the main computational tasks (4 and 5). Tasks 4 and 5 required the majority of the effort and consumed substantial computational resources.

2.1. Task 1: Support JPM Sensitivity Test

Task 1 of RENCI's component of the NC-SLRRIS project provides computational support to Applied Research Associates (ARA) to determine a reduced set of storm tracks for use in the Baseline computation of coastal hazards. To this end, RENCI has conducted ADCIRC simulations on a coarse ADCIRC grid using storm track data provided by ARA. RENCI provided the storm surge results back to ARA for further analysis.

RENCI received two sets of candidate storm tracks from ARA: NC-Reduced-set-1-B-Case and NC-Reduced-set-2-BandC-Case. These sets contain 450 and 294 tracks, respectively. Each set was converted from the ARA "hur" format to the ADCIRC fort.22 format, and the surge response was computed on a coarse grid that covers the North Carolina region and surrounding waters (Figure 1). This grid has 4636 nodes and 8703 elements, does not include land (i.e., does not support land inundation), and executes very fast in a serial computational mode. Maximum surge levels were

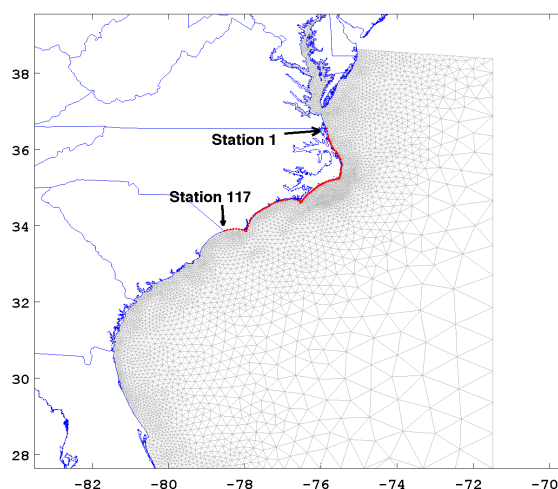


Figure 1: Coarse ADCIRC grid used for storm track selection screening.

recorded at each of 117 coastal nodes in North Carolina (indicated by the red dots in Figure 1). In addition to the two reduced track sets, RENCi also computed the coarse grid surge response to the full NC FIS track set, which contains 675 tropical storms.

Each simulation computes a maximum storm surge, an example of which is shown in **Error! Reference source not found.** for a relatively intense landfalling storm (dp4r3b2c3h1l1). For each “scenario” or set of tracks, the maximum surge results are gathered and the return levels are computed using the Joint Probabilities Method as described by ARA. Figure 3 shows the 1% water level at each coastal node in the coarse grid, with the numbering as indicated above. Changes in coastline orientation and continental shelf width are evident. Compared to the 1% surge levels computed with the full FIS track set (NCFMP_Final_EQSpacing), the rms difference for both reduced sets is 11 cm. This is summarized in the **Error! Reference source not found.**

Table 1: Basic statistics for comparison of surge results from the three track sets. The comparison is made for the 1% return level at the coastal nodes.

	Rms	min	max
Set-1-B-Case	.11	-.29	.27
Set-2-BandC-Case	.11	-.35	.25

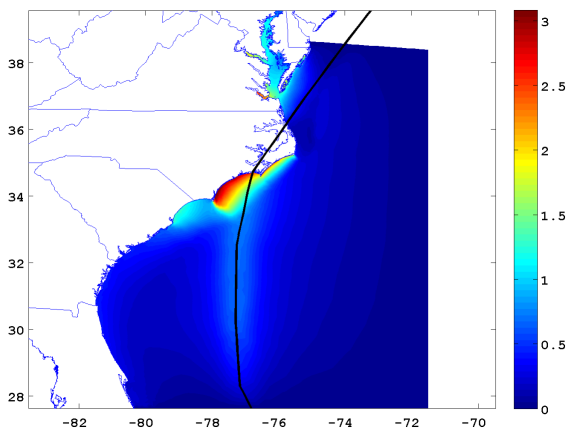


Figure 2: Example of coarse grid surge response to a landfalling storm. The storm track is shown with the black line, and the water level is shown in color in meters.

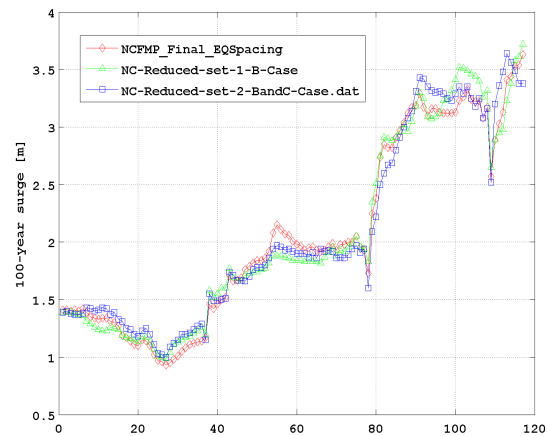


Figure 3: 1% Surge return level at coastal node locations for the storm surge computed from the three track sets. The abscissa is the numbering of the coastal nodes (1-117) as indicated in Error! Reference source not found.

2.2. Task 2: Wind Field Generation

Each tropical storm defined as input to the computational system requires wind and pressure fields to force the models. In this task, RENCI computed the wind and pressure fields associated with each of the 294 tropical storms defined by ARA, using ARA’s HBL wind model. This storm suite was used for the main computational scenarios (baseline, 20 cm, 40 cm, 60 cm, 80 cm, and 100 cm ADCIRC grids).

2.3. Task 3: Tidal Datum Code

Prior to initiation of the RENCI tasks, the explicit task to develop a tidal datum code was removed from the scope. However, this original task is maintained in the scoping and reporting documents to maintain consistent numbering between the task order, proposals, and contracts. The tidal datum code was developed independent of, and external to, the NC-SLRIS project.

2.4. Task 4: Perform Baseline Simulations

A baseline scenario was computed on the first project ADCIRC grid (Version 4.3.2). This scenario reflects the present-day storm climate and the grid is a reduced version of the larger FIS grid. All simulations in this and subsequent SLR scenarios used the coupled ADCIRC+SWAN model, version 49.60. For this present-day scenario, as well as the subsequent SLR scenarios, the following set of activities was performed. Results for the baseline activities are shown in this section. Results from the SLR simulations are shown in Section 2.5 below.

2.4.1 Equilibrium tidal solution

An equilibrium tidal solution was computed on the scenario grid, with the same tidal elevation boundary conditions that were used in the NC FIS tidal validation study (Egbert et al, 1994). The main model outputs from this simulation include the global elevation and velocity harmonic analysis files and a station velocity file. The stations for velocity output were specified across each tidal inlet and river mouth. This output was used by subsequent project analyses. The main simulation parameters are as follows:

Time Step	0.5 sec
Run Length	77.625 days (150 M ₂ tidal cycles)
Rampup Length	10.35 days (20 M ₂ tidal cycles)
Tidal Constituents	M ₂ , S ₂ , N ₂ , K ₂ , K ₁ , O ₁ , P ₁ , Q ₁
Harmonic Analysis Period	Days 10.35 through 77.625

2.4.2 Tidal Datums

Tidal datums were then computed at each ADCIRC grid node from the global harmonic analysis file of the equilibrium tidal solution. This includes the usual tidal datums of Mean Higher High Water (MHHW), Mean High Water (MHW), Mean Low Water (MLW), and Mean Lower Low Water (MLLW), as well as cumulative distributions of tidal heights needed for the subsequent JPM and EST statistical analyses. GIS-compatible files for each datum were also produced.

Each surface is initially defined only over water, since the harmonic analysis results are sensitive to the percent of time that a node is wetted during the harmonic analysis period. In order to use the tidal datums over land for the surge statistical analyses, the datum surfaces are extended inland to cover the areal extent of the surge results. The datums are computed in MSL and converted to NAVD88 as the last step in the analysis. Figure 4 shows MHHW and MLLW water levels above NAVD88 for the baseline scenario.

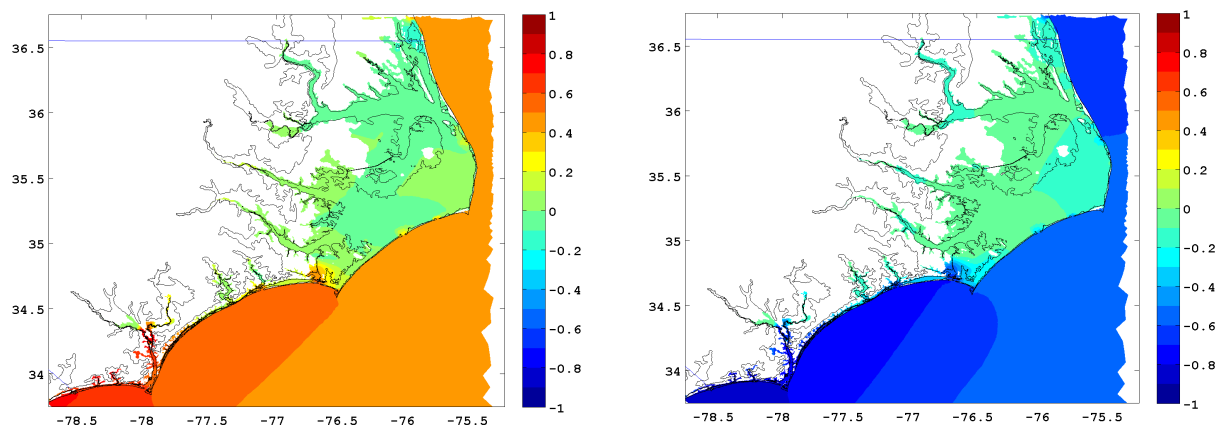


Figure 4: Tidal datums from baseline scenario equilibrium tidal simulation. Left) Mean Higher High Water (MHHW). Right) Mean Lower Low Water (MLLW). Units are meters relative to NAVD88.

The computed datum values were compared to the NOAA-published values (Table 2). The NOAA values are published relative to the station datum, so the MSL level has been subtracted from the NOAA values for comparison to the computed datums, which are relative to ADCIRC’s mean sea level. Overall, the computed tidal datums are within 2-6 cm of the observed values.

Table 2: Tidal Datum Comparison for Baseline Equilibrium Tidal Solution. Units are meters relative to MSL.

	NOAA	ADCIRC	NOAA	ADCIRC
	MHHW-MSL	MHHW	MLLW-MSL	MLLW
Duck, NC	0.58	0.59	-0.54	-0.51
Oregon Inlet Marina, NC	0.18	0.21	-0.18	-0.18
Cape Hatteras Fishing Pier, NC	0.56	0.55	-0.49	-0.46
Beaufort, NC	0.56	0.59	-0.52	-0.51
Wilmington, NC	0.68	0.72	-0.74	-0.69
Wrightsville Beach, NC	0.69	0.71	-0.62	-0.62
Southport, NC	0.74	0.74	-0.71	-0.66
Sunset Beach, NC	0.87	0.83	-0.81	-0.76

2.4.3 Simulation of Historical Hurricanes

Two historical events (Fran 1996; Isabel 2003) were simulated. These simulations included tides, with a 45-day tidal spinup period prior to the onset of the wind and pressure forcing, and starting equilibrium adjustment factors for the specific start date. The maximum water level and wave heights were retained for visualization as well as other project analyses.

Table 3: Start and end times for the validation simulation components, and run lengths in days.

Storm	Tidal Start Date	Met Start Date	Simulation End Date	Met length, Total Run Length [days]
Fran (1996)	1996-07-16 00Z	1996-08-30 00Z	1996-09-07 00Z	7.8, 52.8
Isabel (2003)	2003-07-31 00Z	2003-09-14 00Z	2003-09-19 12Z	5.5, 50.5

The maximum water levels from the two historical tropical storm simulations are shown in Figure 5. Hurricane Fran maximum water levels are largest along the coast from Wrightsville Beach southward to Frying Pan Shoals, with the highest levels reaching 3.25 meters. Cape Fear River levels are about 1.0 to 1.25 meters. Hurricane Isabel caused larger inland effects, mainly in the Pamlico Sound area, with the maximum later levels generally in the lower Neuse River. These solutions were compared to the observed high water marks that were analyzed for the NC FIS. The error distributions are shown in Figure 6. Both solutions are relatively skillful, with rms errors of 0.38 and 0.30 meters, and are consistent with the validation results from the NC FIS.

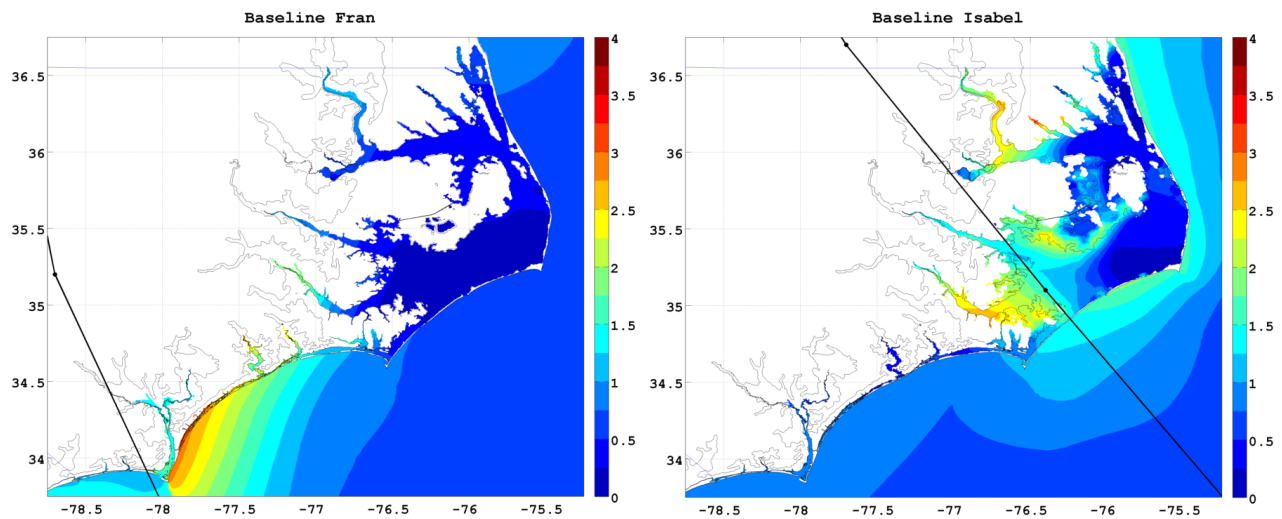


Figure 5: Historical simulation maximum water level for the baseline (present-day) scenario for Hurricanes Fran (1996) and Isabel (2003). The storm tracks are shown with the black line. Water level units are meters NAVD88.

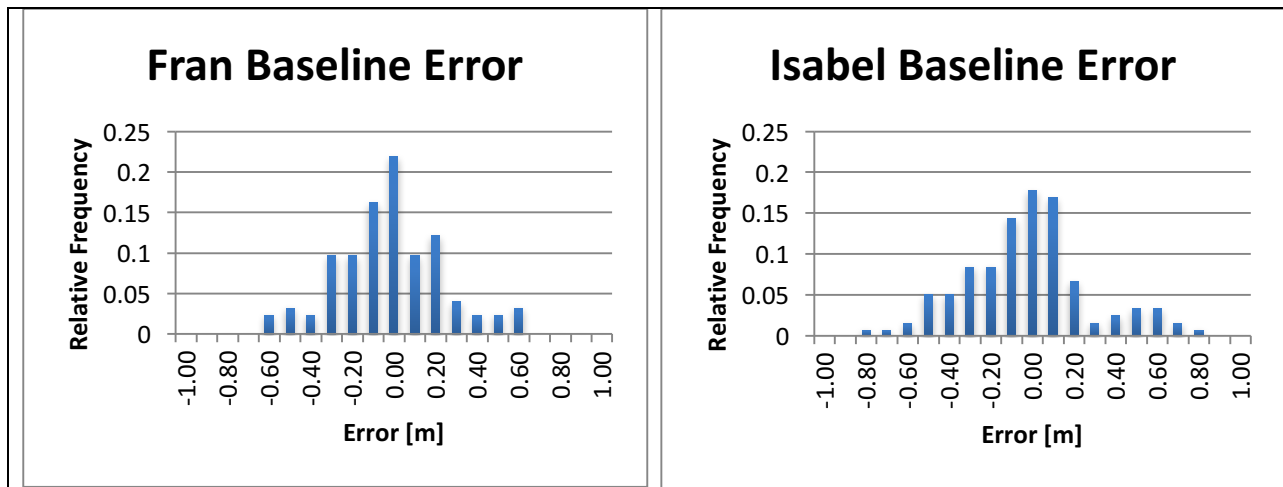


Figure 6: Error distribution for historical baseline simulations. Left) Hurricane Fran (1996). The rms error is 0.38 m. Right) Hurricane Isabel (2003). The rms error is 0.30 meters.

2.4.4 Production storm surge simulations

The production storm surge simulations are the main computational step in the baseline and SLR scenario. This step carried out the production tropical and extratropical storm simulations required for the EST and JPM return period analyses. Generally, the extratropical storms were run first in order for the EST statistical processing to occur concurrently with the tropical storm simulations. The combined number of storm simulations (294 tropical + 21 extratropical = 315) took about 4 weeks to compute. An overview of the production simulation results is shown next. The ranked storm surge values are shown in Figure 7 for three coastal locations. Both extratropical and tropical storms are included. Generally, the extratropical storm surges are of larger magnitude north of Cape Hatteras (Duck). The 1993 extratropical storm caused significant surges in the Cape Fear River, seen as the green circle at about storm number 275. The maximum of all storm maxima is shown in Figure 8. The largest values exceed 5 meters along the coast in the Wrightsville Beach area, with 3+ meters in the lower Cape Fear, upper Neuse, New and White Rivers. Since these are the maximum water levels reached across all storms, they represent annual occurrence levels near 0.1% (1 in 1000 years).

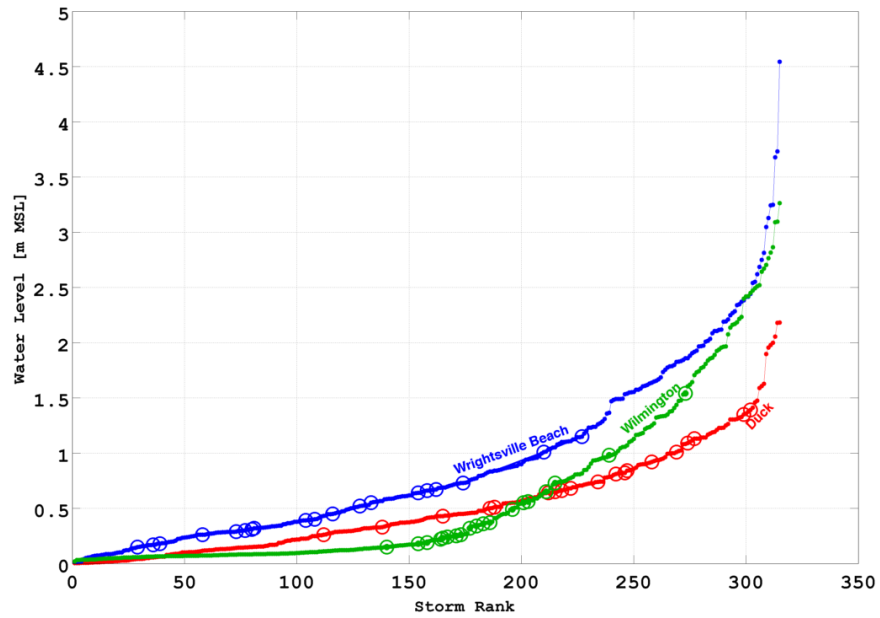


Figure 7: Ranked storm surges for three coastal locations for the baseline production simulations. Circles mark the extratropical simulation results. There are 315 total storms in the storm population.

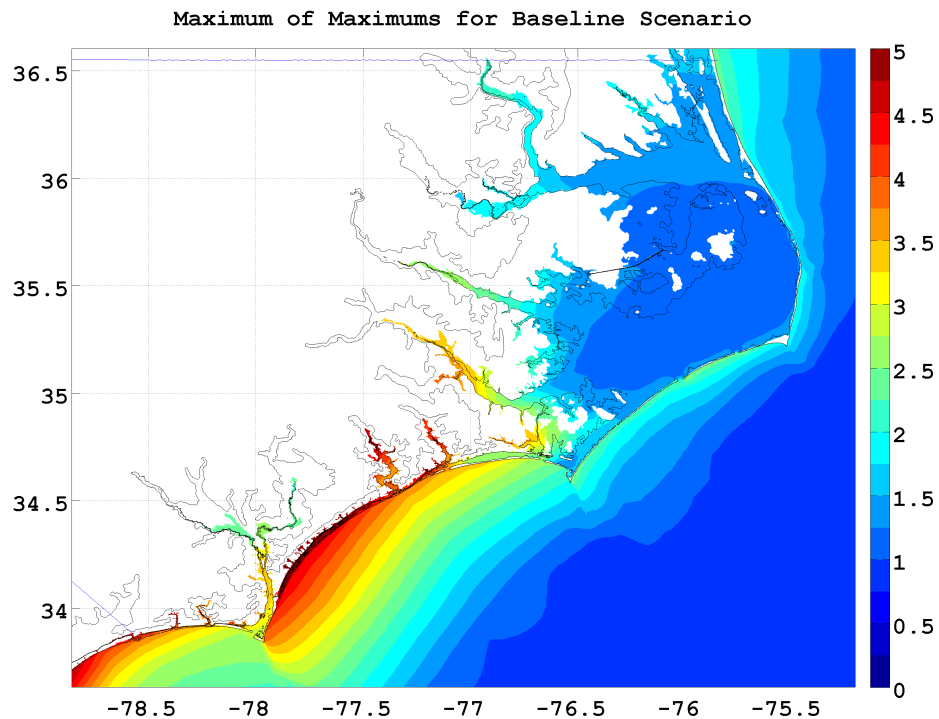


Figure 8: Maximum at each ADCIRC node across all baseline simulations. Units are meters NAVD88.

2.4.5 Statistical synthesis

The final step is the statistical synthesis of the tropical and extratropical results, where the JPM probabilities are used with the tropical production simulation results to compute the water levels associated with the 10%, 4%, 2%, 1%, .2%, and .1% annual chances of occurrence. Likewise, the Empirical Simulation Technique (EST) is used to derive return levels at the same frequencies. All EST analyses were carried out at Dewberry. The final return levels are a statistical combination of the (independent) JPM and EST results. All statistical methods used are consistent with the NC FIS, and each (JPM, EST, combinations, and incorporation of tides) are fully described in prior project documents, the NC FIS IDS #3 document, as well as the EST User's Guide (Scheffner et al, 1999). The final data set from this step is the combined (JPM+EST) return levels for the 10%, 4%, 2%, 1%, .2%, and .1% annual chances of occurrence.

Summary results are shown in Figure 9. The left panel shows the 1% water level for the North Carolina coastal waters. The color scale maximum is set to 5 meters for easier comparison to water levels for the SLR scenarios described below. Water levels are highest along the open coast in the Wrightsville Beach area and lowest in the sounds. The Neuse River levels are higher than the sound levels, consistent with the FIS results. The right panel shows the annual chance levels at Duck, Wrightsville Beach, and Wilmington nodes.

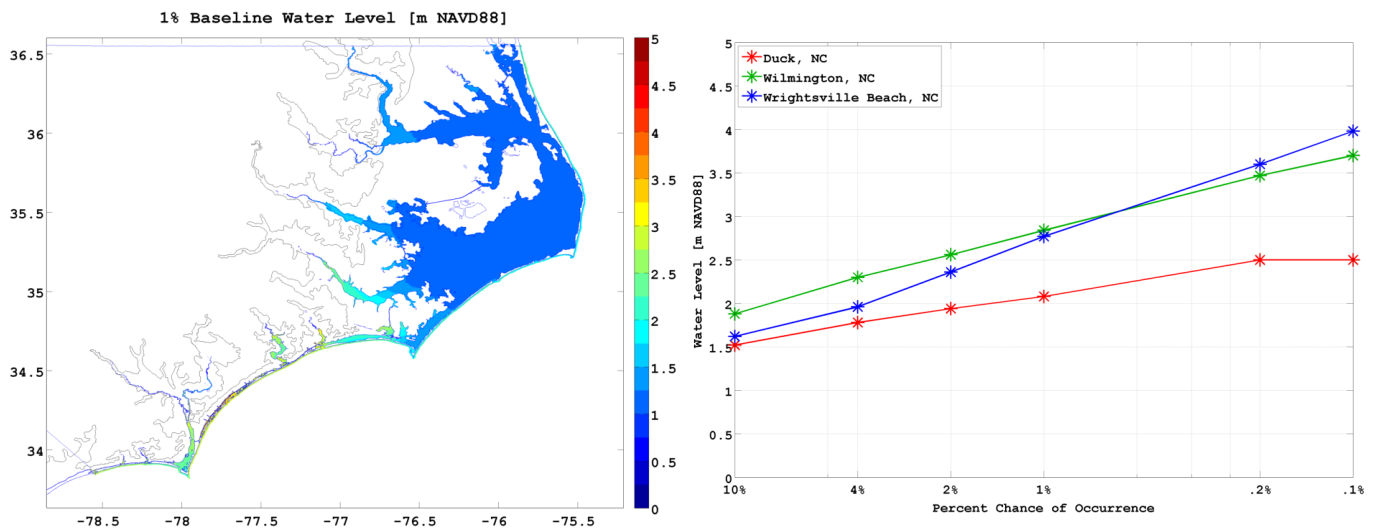


Figure 9: Left) 1% water level (m NAVD88) for the baseline scenario. Right) Water levels at standard occurrence frequencies at three locations.

2.5. Task 5: Perform Sea Level Rise Scenario Simulations

The sea level rise scenarios were computed in the same manner as the baseline (Task 4) scenario. In addition to the equilibrium tides, historical storms, production simulations, and statistical synthesis, one additional step was carried out. In order to determine geomorphological changes for a scenario's ADCIRC grid, RENCI conducted an equilibrium tidal simulation on the previous scenario's grid but with the current scenario's SLR amount; in other words, the effect of the SLR amount on the tides on the previous geomorphological configuration/grid. Tidal datums and tidal velocities across the region's tidal inlets were computed and provided to Dewberry for further application to the scenario's ADCIRC grid.

Each project sea level rise amount (20, 40, 60, 80, 100 cm) represents a "loop" through the baseline procedure. The maximum storm surge surfaces for the historical storms are shown first, and then 1% surface and the return levels at the three selected coastal locations are shown in Figure 10 through Figure 14.

The historical storm results show the generally expected behavior of increased water levels along the open coast in the areas where the storms had the largest impacts. The surge impacts in the land area between Pamlico and Albemarle Sounds becomes increasingly flooded as MSL increases, with water levels reaching 1.5 meters for Fran (1996). For example, this area floods in the 100 cm case and has water levels at about the 1% level (compare the Fran water level and 1% water level in Figure 14). This area does not flood in the baseline through 40 cm cases.

Open-coast water levels tend to increase at amounts consistent with the increased sea level. Physically, this is because the average water depth and continental shelf width do not change appreciably as the mean sea level increases. Since the mean depth and shelf width are the primary factors that control regional surge response, and there is little change in the depth and shelf width, surge increases essentially linearly with the mean sea level increase. In the sheltered waters, however, the simple linear response seen along the open coast is not expected, generally due to nonlinear effects. Particularly, the areal extent of land below mean sea level increases rapidly as mean sea level increases, and thus the lower-lying, flatter areas (e.g., land west of Pamlico Sound) exhibit substantially increased inundation in the end-member scenario (100 cm).

2.5.1 20 cm Scenario:

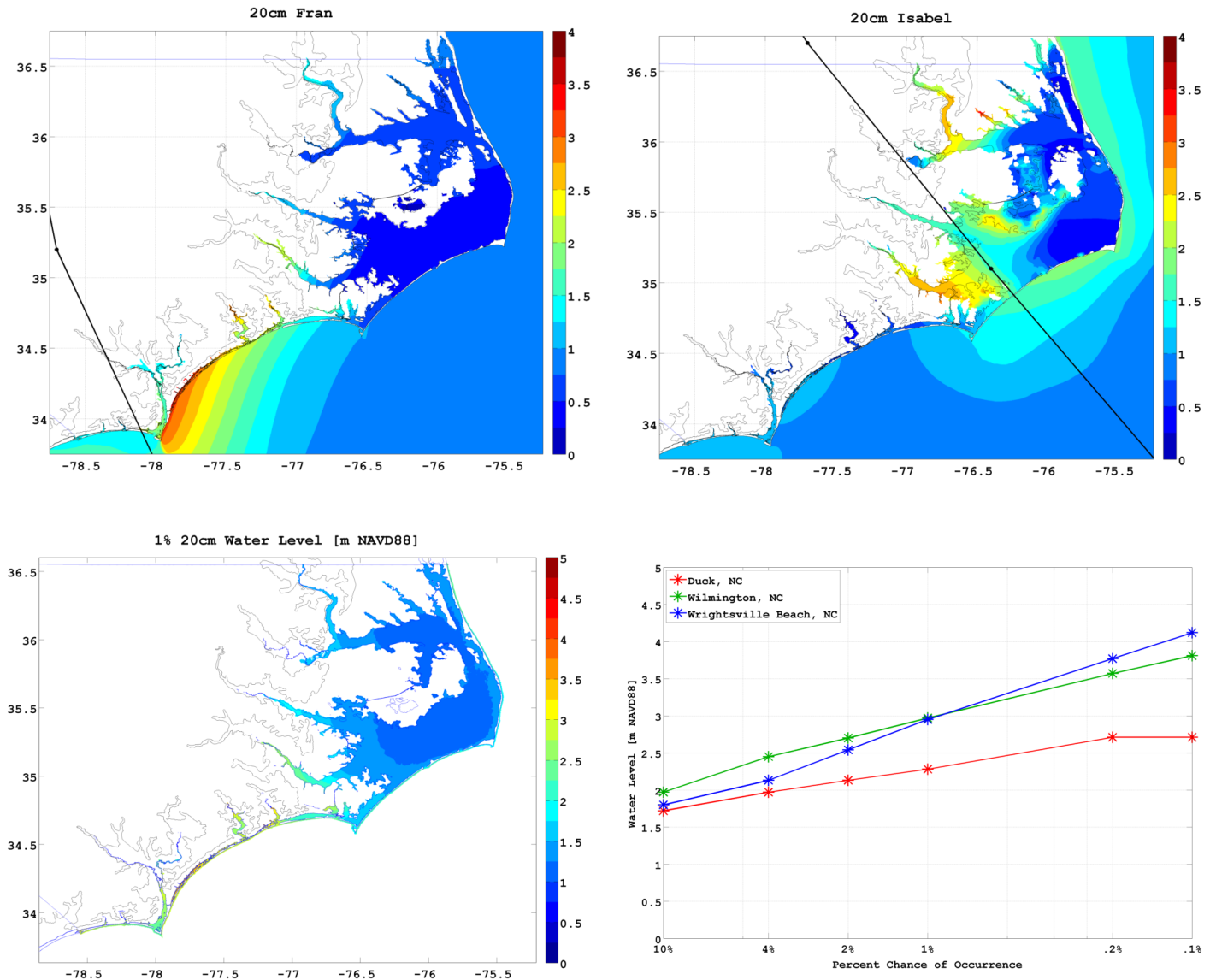


Figure 10: 20cm scenario historical storm maximum surge, 1% combined water level, and return levels for the three selected station locations.

2.5.2 40 cm Scenario:

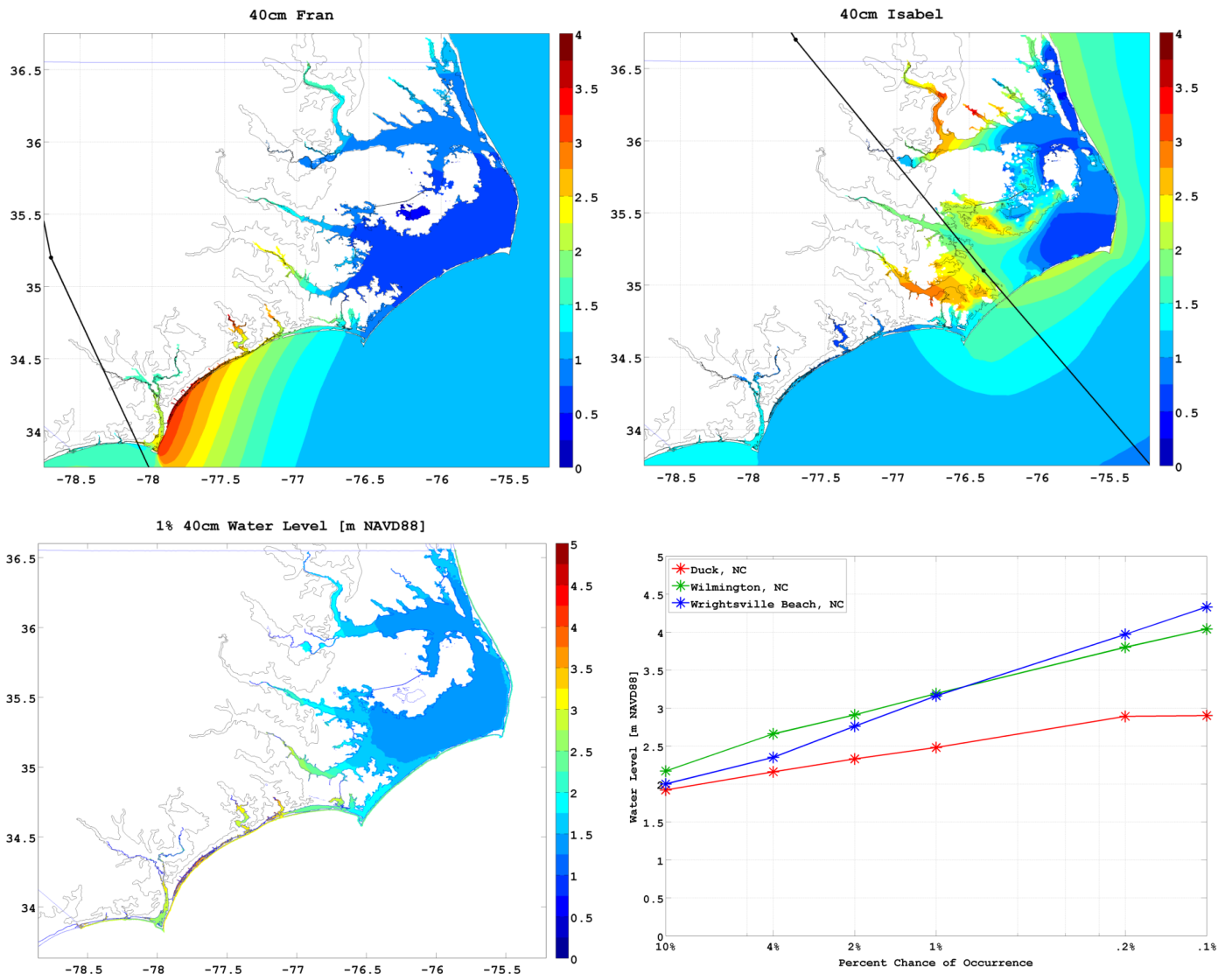


Figure 11: 40cm scenario historical storm maximum surge, 1% combined water level, and return levels for the three selected station locations.

2.5.3 60 cm Scenario:

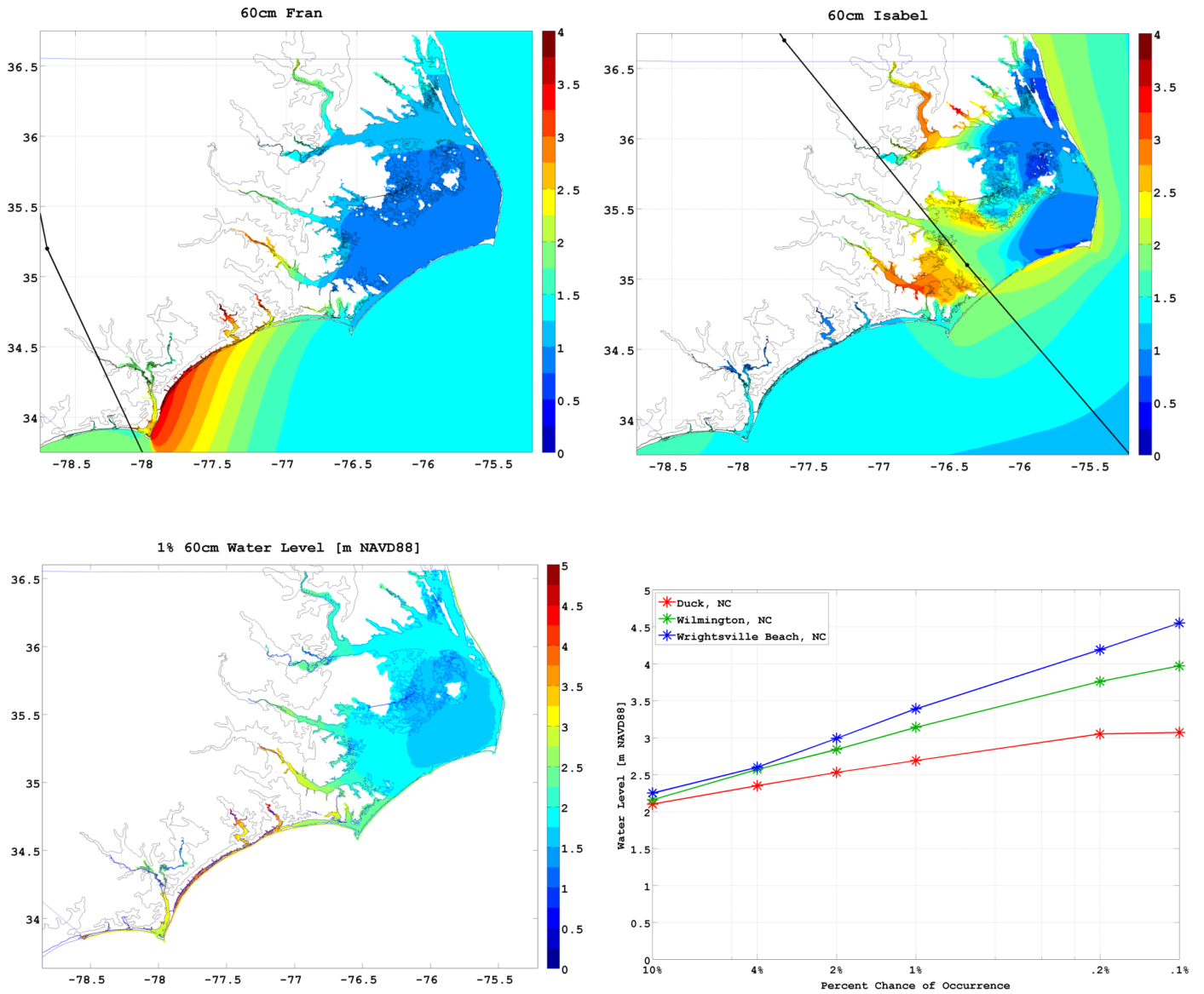


Figure 12: 60cm scenario historical storm maximum surge, 1% combined water level, and return levels for the three selected station locations.

2.5.4 80 cm Scenario:

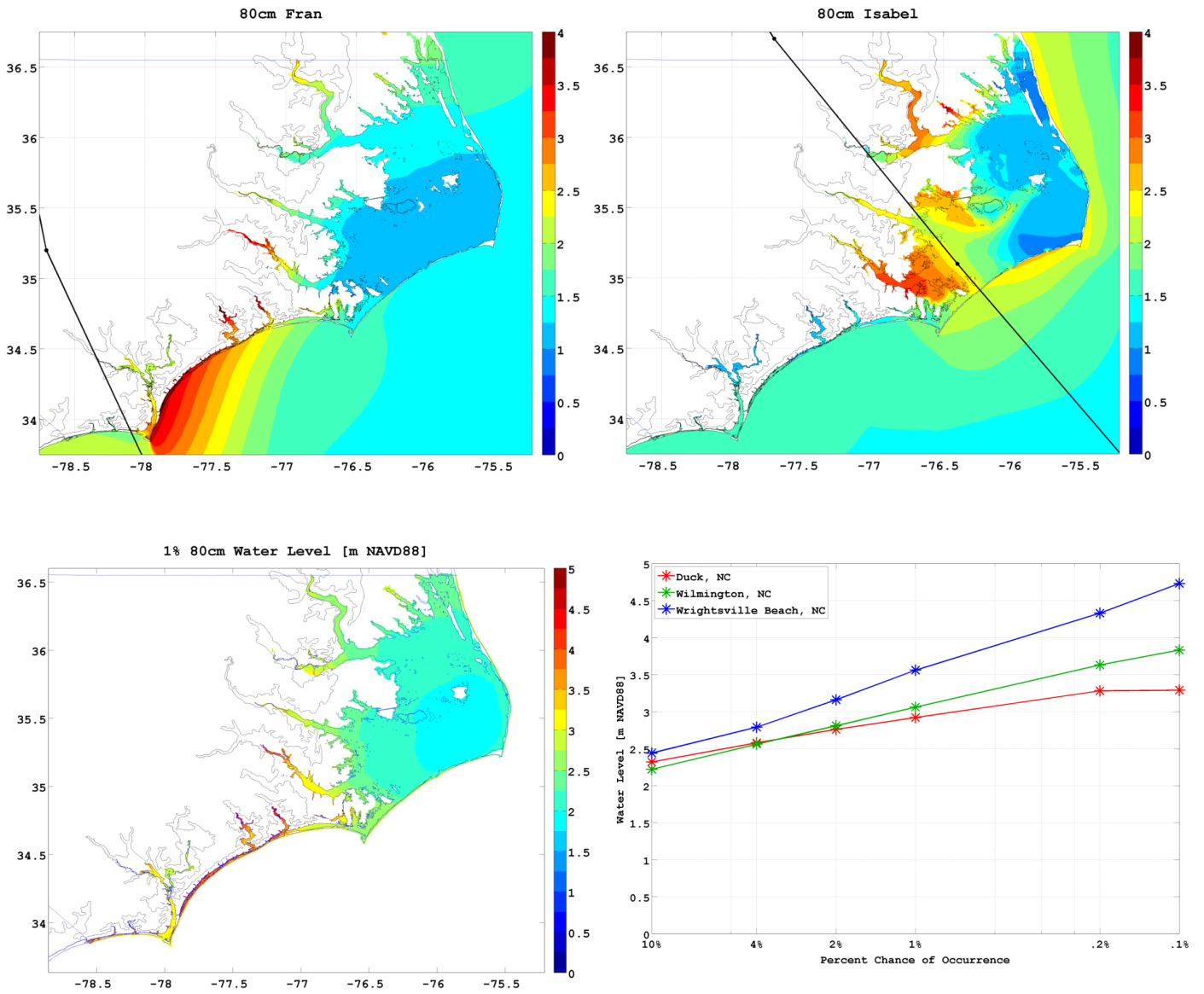


Figure 13: 80cm scenario historical storm maximum surge, 1% combined water level, and return levels for the three selected station locations.

2.5.5 100 cm Scenario:

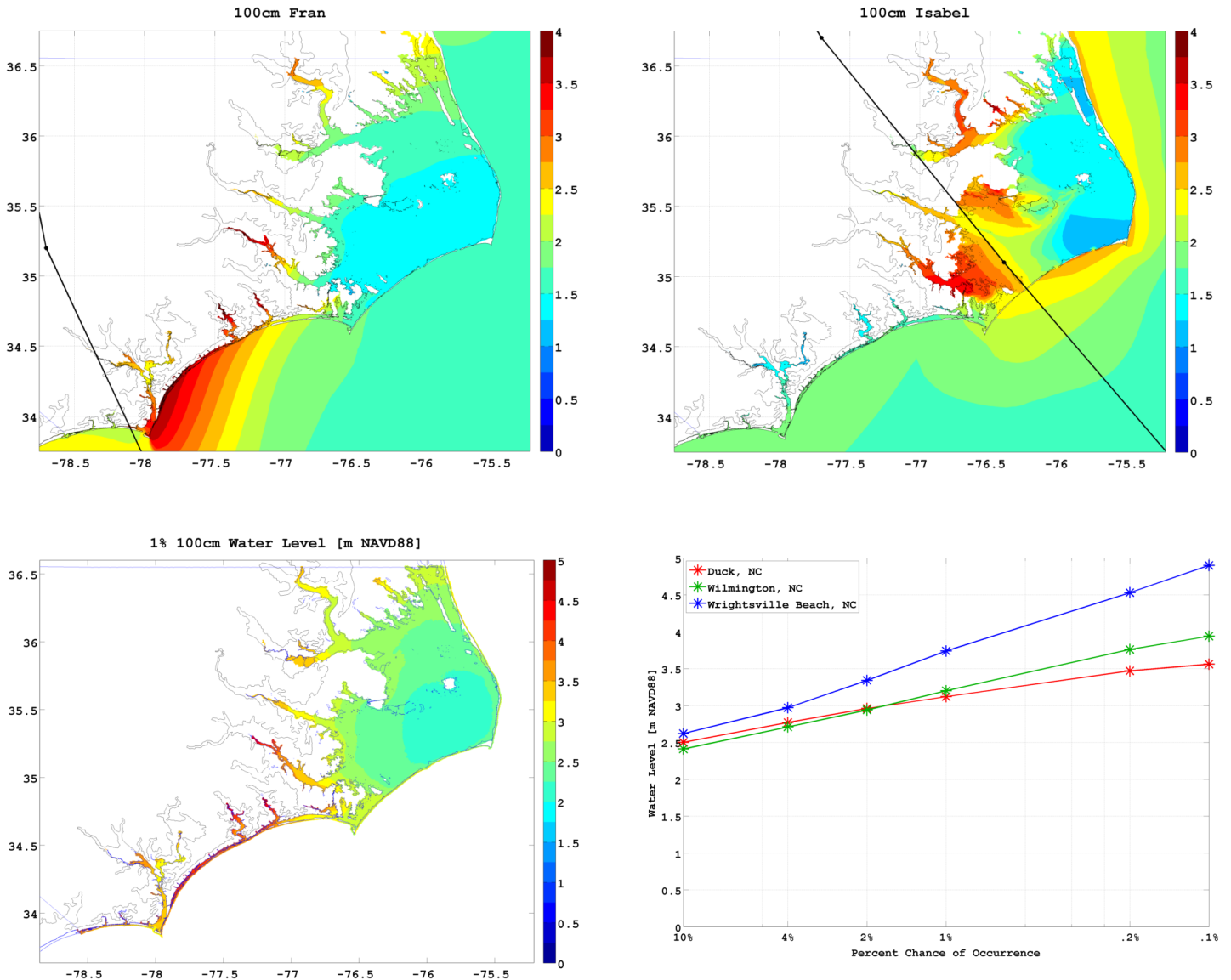


Figure 14: 100cm scenario historical storm maximum surge, 1% combined water level, and return levels for the three selected station locations.

2.6. Task 6: Storminess statistical analyses

The effects of possible changes in tropical cyclone are incorporated into the scenario statistical syntheses by reweighting the JPM storm weights. No additional or different storm simulations (either wind/pressure or ADCIRC simulations) were required. The reweighting procedure and results is described elsewhere in the project documentation. ARA provided two sets of revised storm weights; Set A for the mid 21st century, and Set B for the end 21st century. For each combination of SLR scenario and storminess set in Table 4, numbered 1-9, the JPM return levels were recomputed using the revised storm weights and the previously computed surge results from the SLR scenario. Results for the 1% surface and the return levels at the three selected coastal locations are shown below, for each of the storminess scenarios, in Figure 15 through Figure 23.

Table 4: Storminess and scenario combinations.

Storminess Application			
Value, m	Time Frame	a	b
0	2010-2100		
0.1	2050-2100		
0.2	2050-2100	1	
0.3	2075-2100		
0.4	2100	2	3
0.6	2100	4	5
0.8	2100	6	7
1	2100	8	9
Storm Set a:		Mid 21 st century	
Storm Set b:		End of 21 st century	

2.6.1: 20 cm SLR and Mid 21st Century:

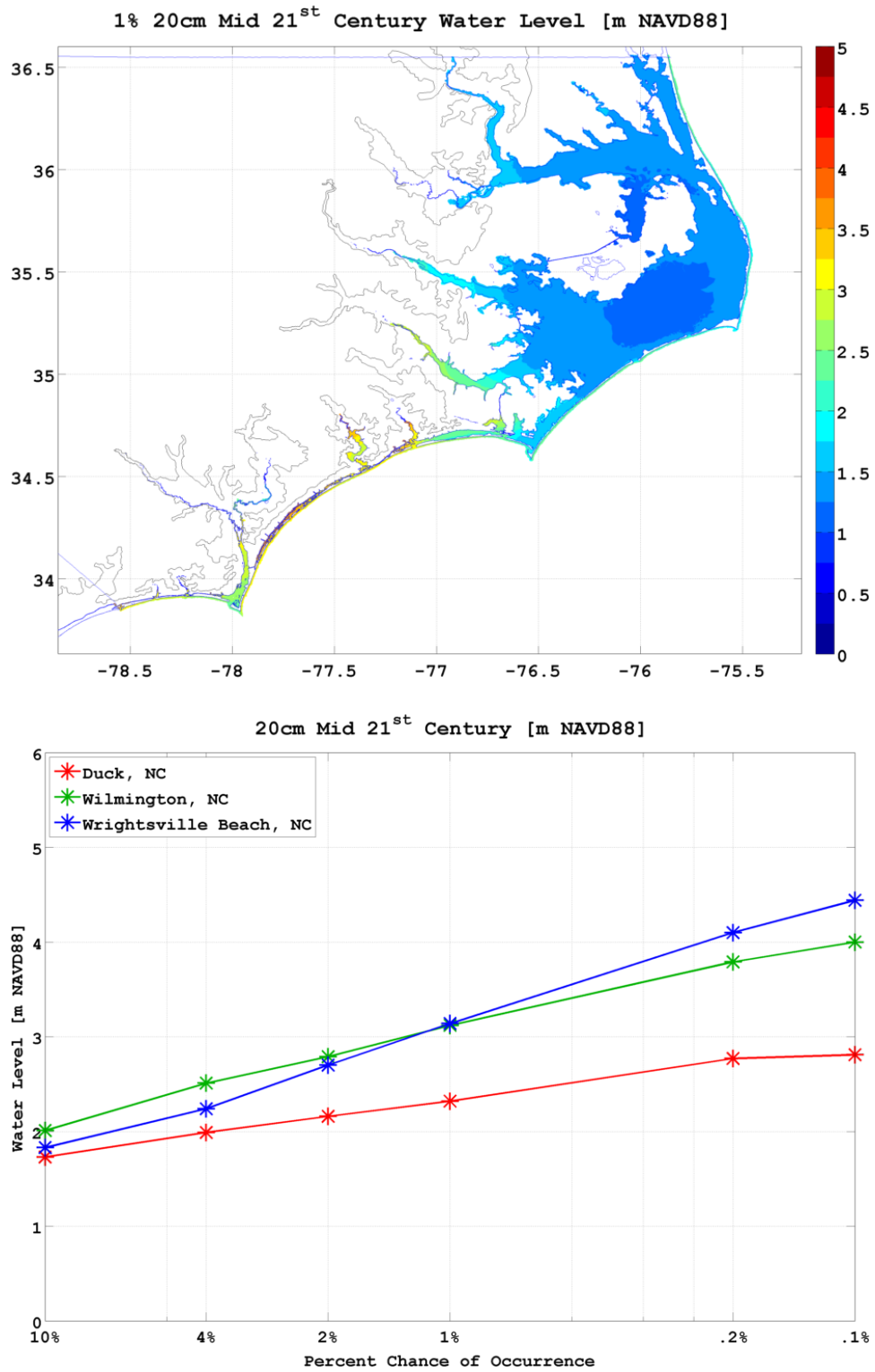


Figure 15: 1% water level and return levels for storminess combination 1 of 20 cm SLR and mid-century storm climate.

2.6.2: 40 cm SLR and Mid 21st Century:

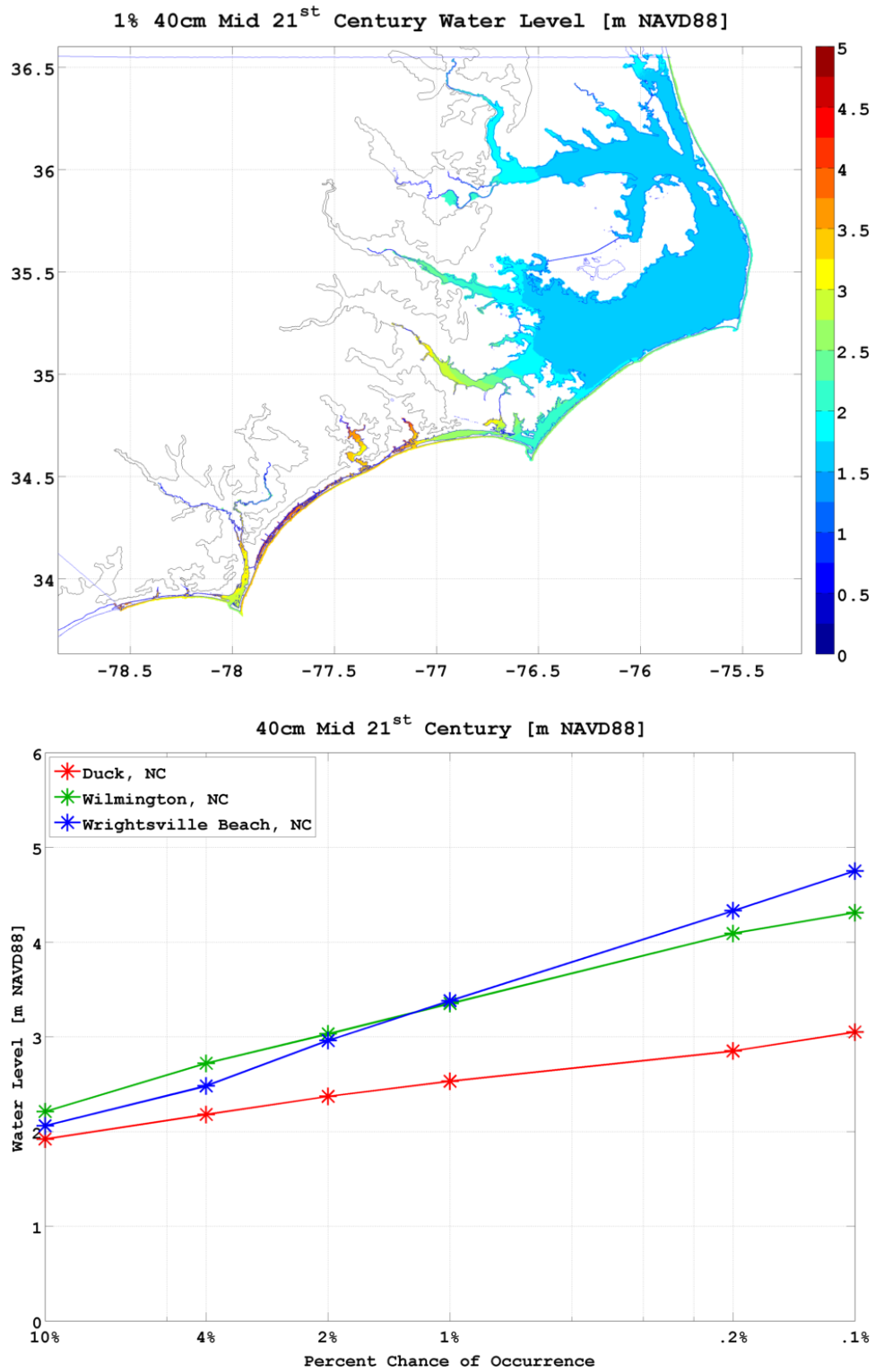


Figure 16: 1% water level and return levels for storminess combination 2 of 40 cm SLR and mid-century storm climate.

2.6.3: 40 cm SLR and End 21st Century:

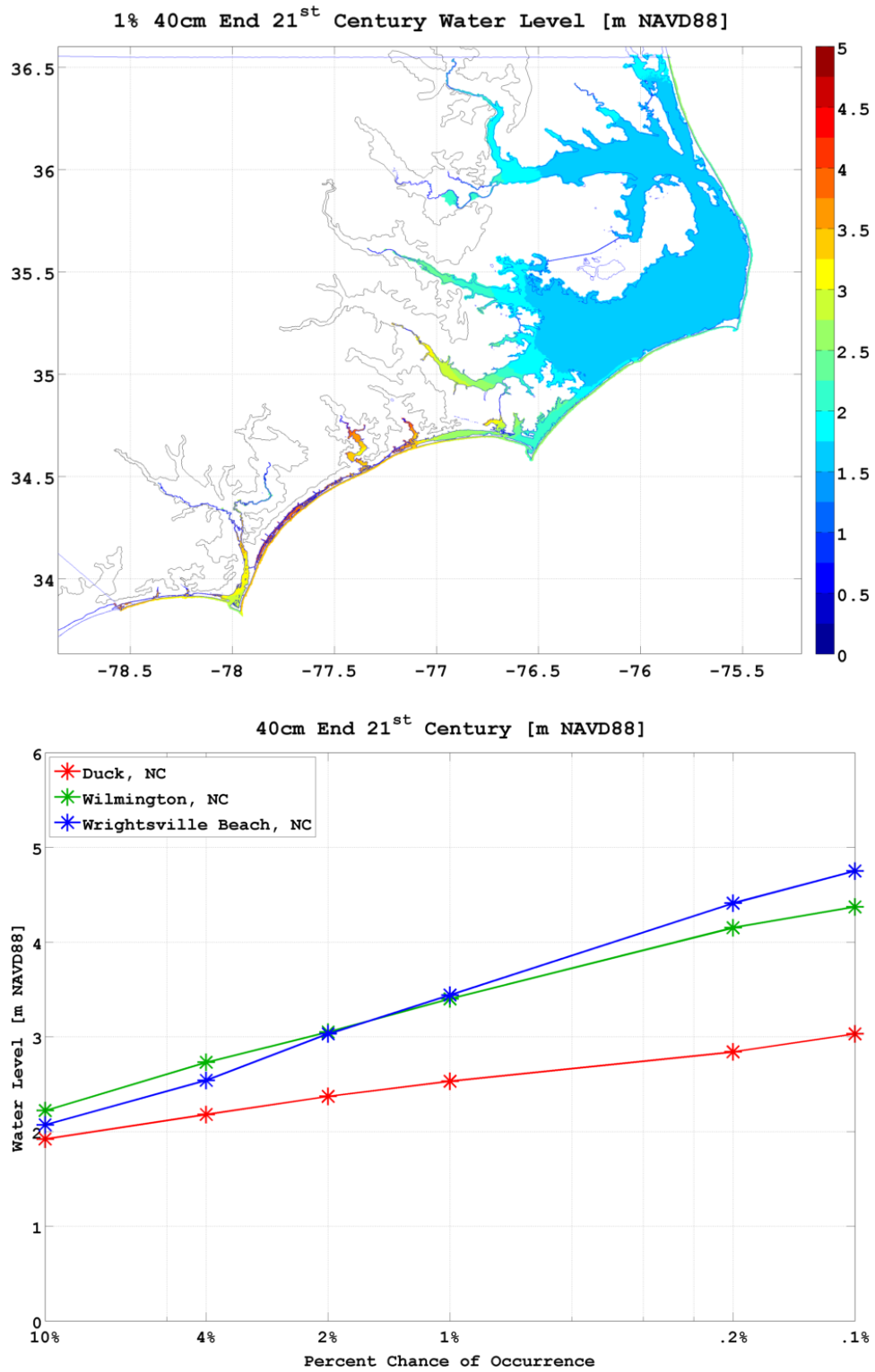


Figure 17: 1% water level and return levels for storminess combination 3 of 40 cm SLR and end-century storm climate.

2.6.4: 60 cm SLR and Mid 21st Century:

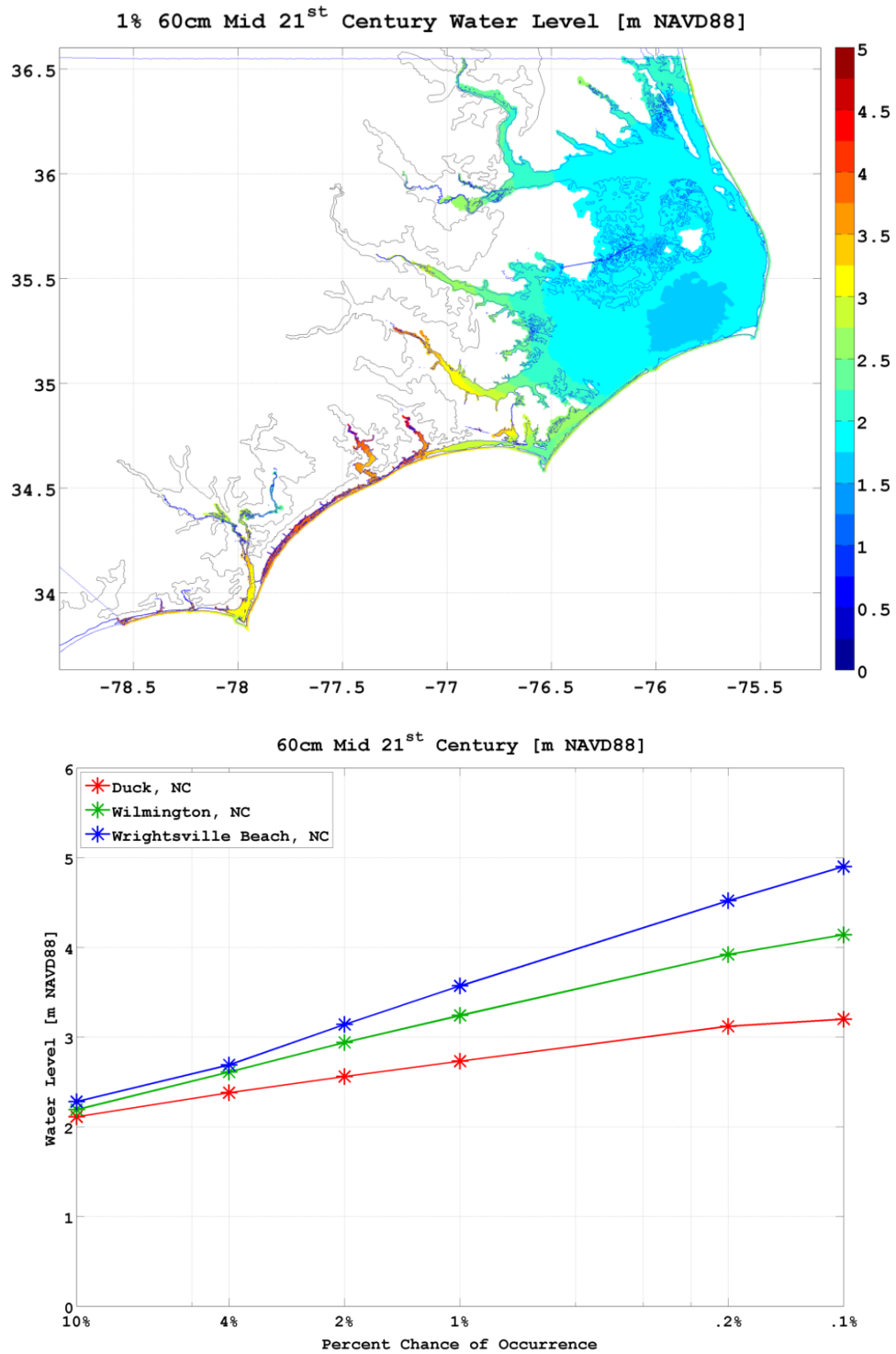


Figure 18: 1% water level and return levels for storminess combination 4 of 60 cm SLR and mid-century storm climate.

2.6.5: 60 cm SLR and End 21st Century:

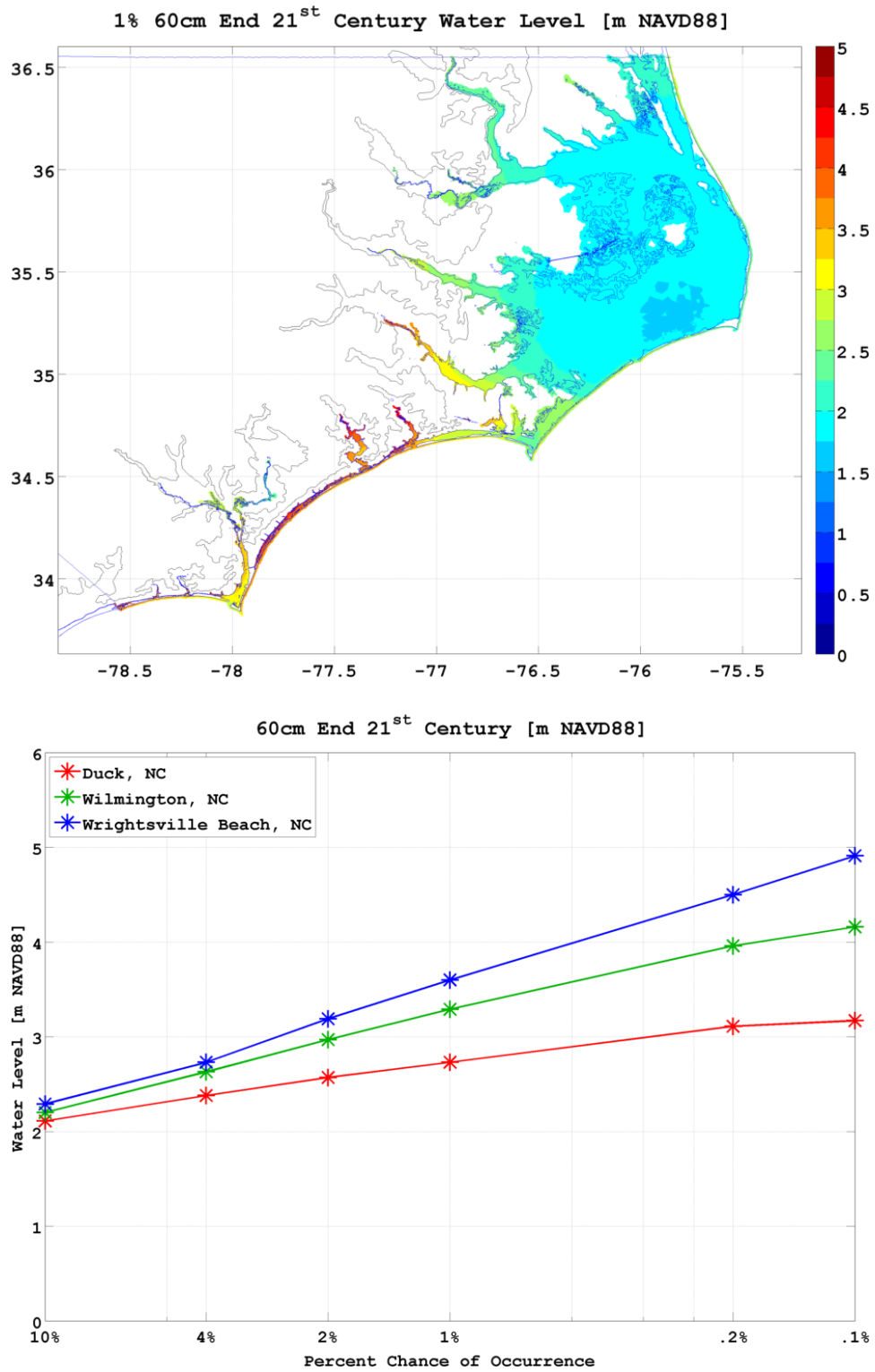


Figure 19: 1% water level and return levels for storminess combination 5 of 60 cm SLR and end-century storm climate.

2.6.6: 80 cm SLR and Mid 21st Century:

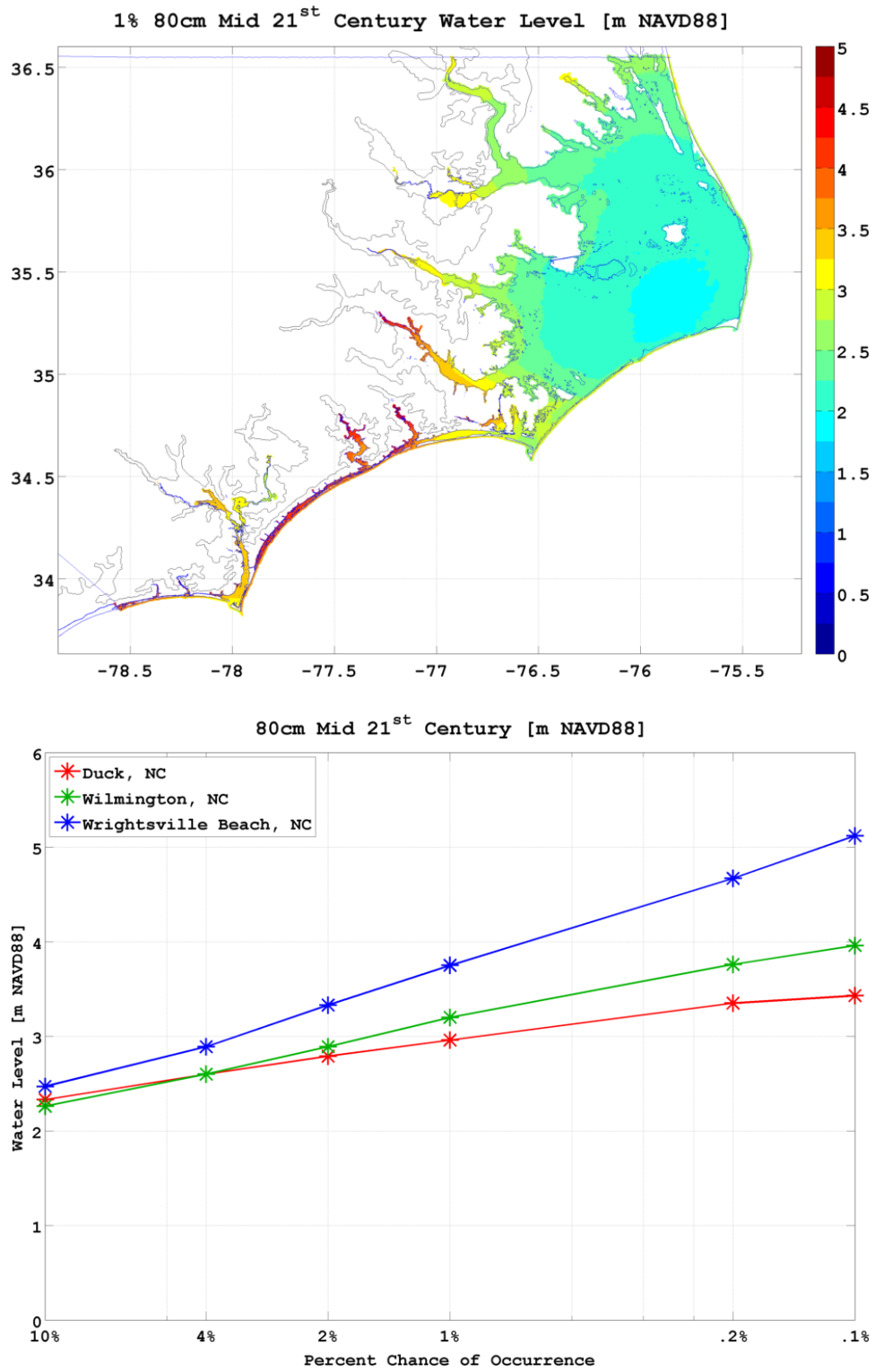


Figure 20: 1% water level and return levels for storminess combination 6 of 80 cm SLR and mid-century storm climate.

2.6.7: 80 cm SLR and End 21st Century:

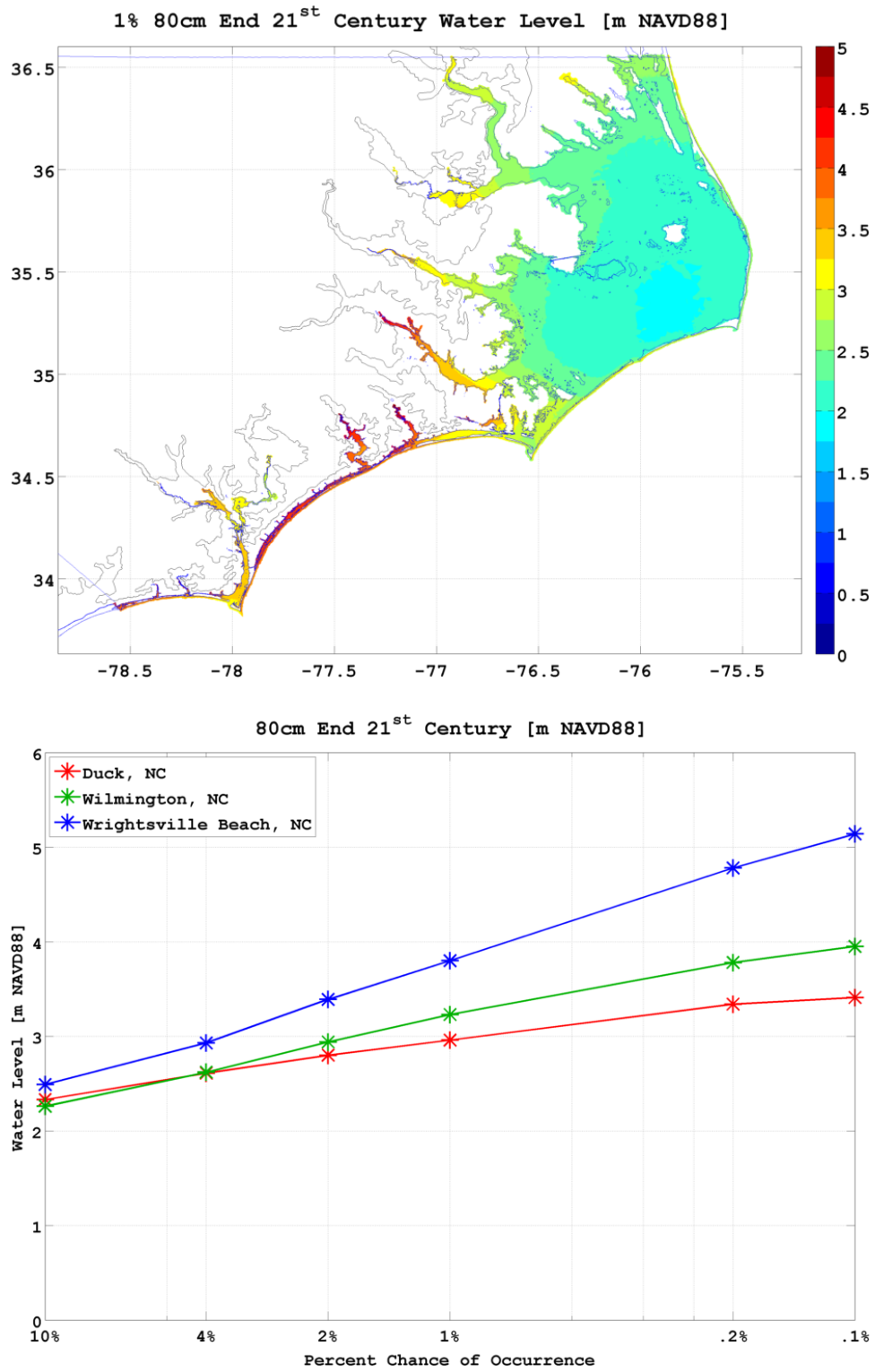


Figure 21: 1% water level and return levels for storminess combination 7 of 80 cm SLR and end-century storm climate.

2.6.8: 100 cm SLR and Mid 21st Century:

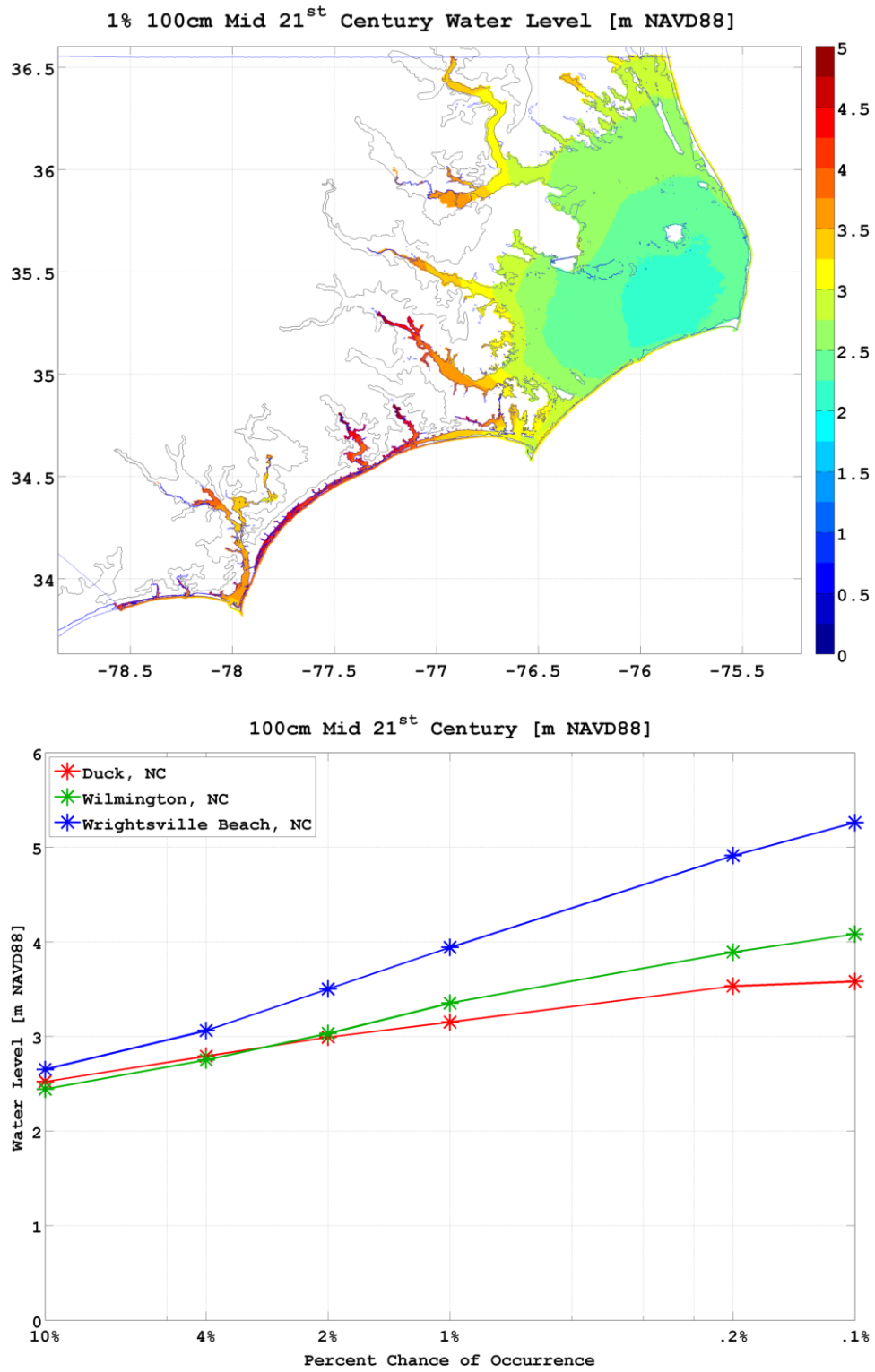


Figure 22: 1% water level and return levels for storminess combination 8 of 100 cm SLR and mid-century storm climate.

2.6.9: 100 cm SLR and End 21st Century:

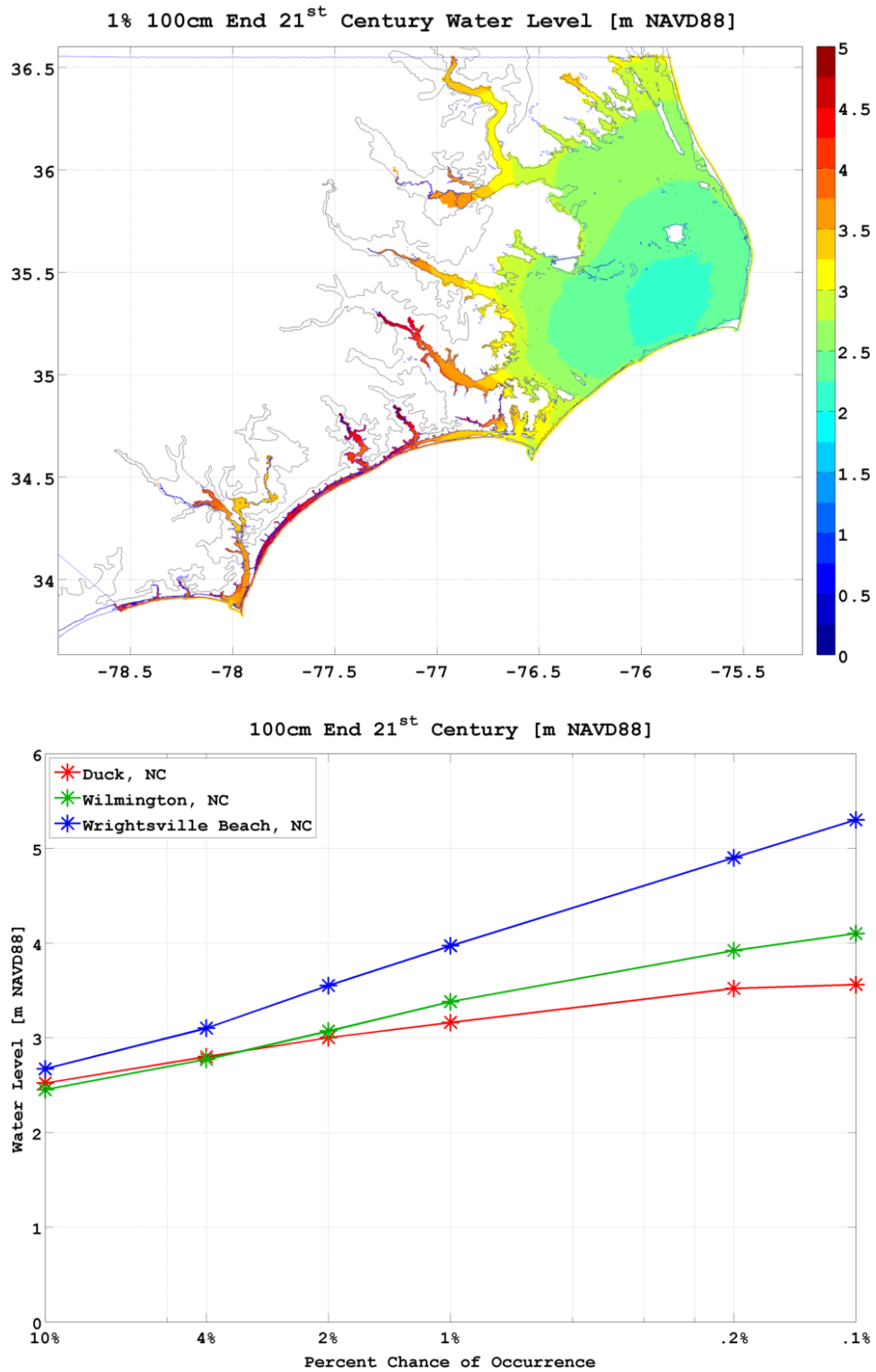


Figure 23: 1% water level and return levels for storminess combination 9 of 100 cm SLR and end-century storm climate.

2.7. Overview of statistical results

The following figures show the return levels for the different scenarios for each station separately. The Duck and Wrightsville locations are representative of the open coasts north and south of Cape Hatteras, respectively. For the SLR scenarios (Figure 24), return levels are generally lower, for a specific recurrence frequency, along the Outer Banks, and the increase in water level at lower frequencies is less. This is due primarily to the relatively smaller impact of the tropical storm surges results in the combined water levels. Essentially, the opposite occurs in the lower part of the NC coastal waters; water levels at specific frequencies are larger than those in the Outer Banks, and levels increase more as the frequency decreases. The water level behavior at Wilmington is complex and discussed further in Section 3.

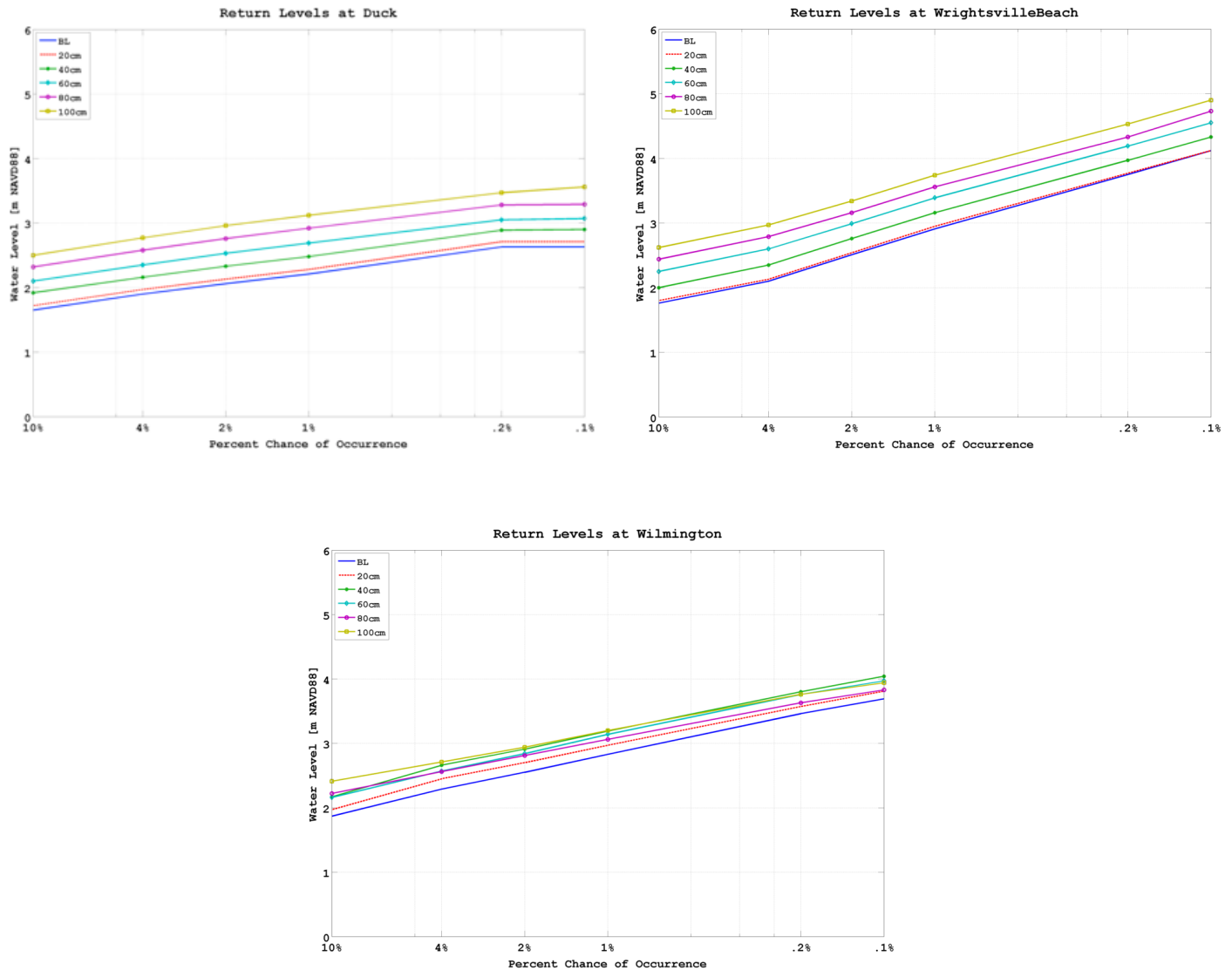


Figure 24: SLR Scenario return levels at the three model nodes for Duck, Wrightsville Beach, and Wilmington.

Figure 25 shows the return levels for the storminess scenarios. Generally, the qualitative results are similar to the SLR scenarios in terms of the behavior north and south of Cape Hatteras, as well as in the upper Cape Fear. The impacts of the storminess JPM modifications are most notable at the Wrightsville Beach location, where the return levels at lower frequencies are higher than those for the present-day storm climate (as shown in Figure 25).

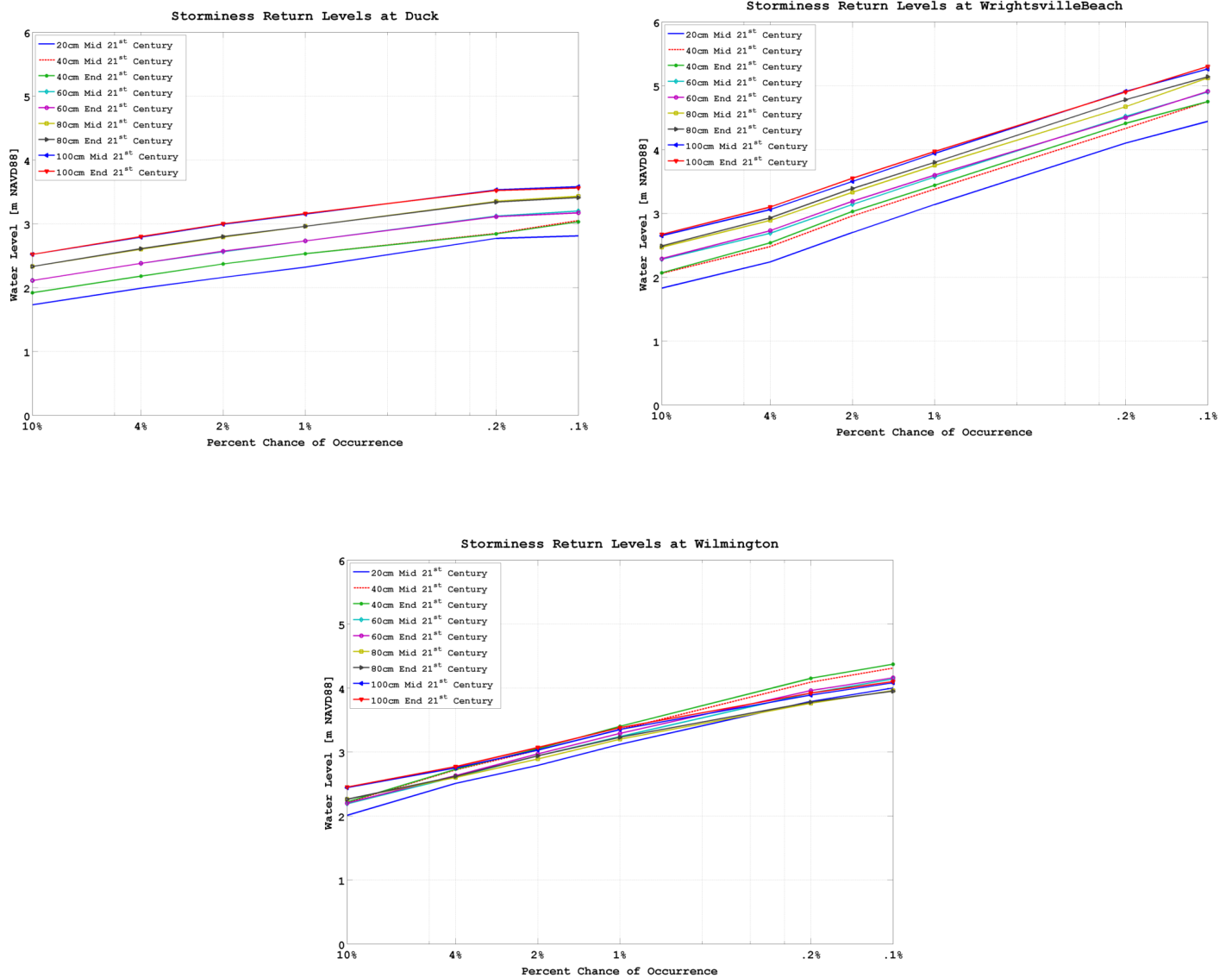


Figure 25: Storminess Scenario return levels at the three model nodes for Duck, Wrightsville Beach, and Wilmington.

3. CAPE FEAR WATER LEVELS

During analyses of the NC-SLRIS model-generated products for the statistical flood elevation surfaces, it is noticed that, in the Wilmington area, SWEL values do not increase in proportion to the increased MSL increment imposed on the scenario. This area is of particular concern given the placement of a NOAA tide gauge near the turning basin and the data analysis of the water level record in the context of channel dredging activities and tidal amplitudes.

At face value, smaller increases in SWEL than expected seem problematic and concern was placed on RENC1's numerical model results. This unexpected behavior is shown in Figure 26 for the JPM results, along approximately equidistant points from the river mouth (0 km) to about 30 km upstream of Wilmington, taking the westward channel branch to the west of Eagle Island.

The upper plot shows the 1% SWEL values along the Cape Fear River including tides and the error term from the NC FIS project. The lower plot shows the JPM levels without the tidal and error contributions. Considering first the JPM+Tides+Error results, the 1% values increase by about the sea level increase at the river mouth. As the scenario "increases", the water levels increase in the lower river region, but do not increase as much as expected upstream of the Wilmington area (at about 45 km from the river mouth). Additionally, It appears that the 40 cm water levels are actually larger than the 3 later scenarios, at least in a limited region near Wilmington.

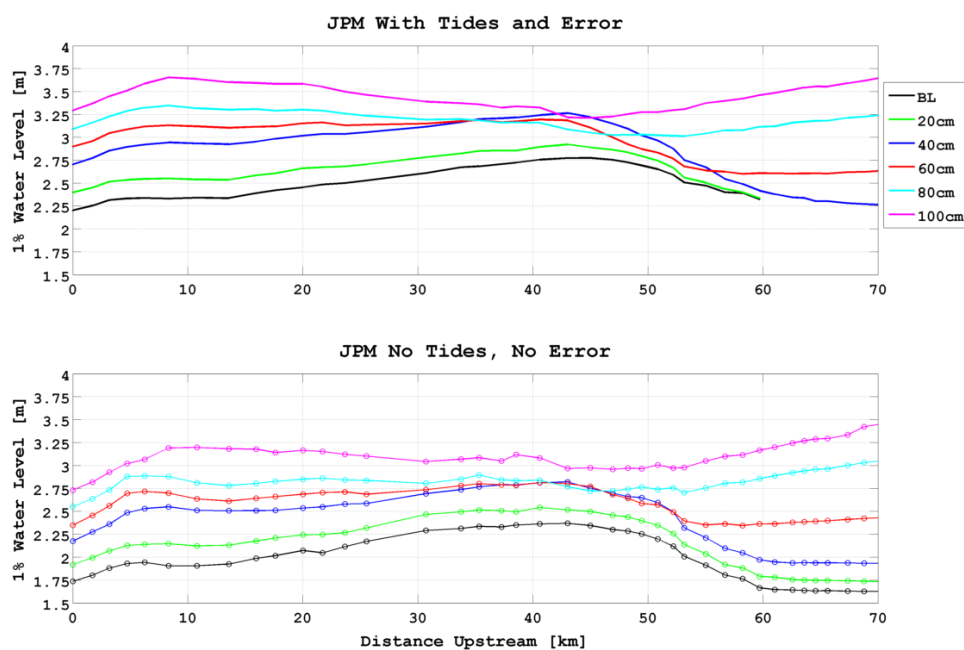


Figure 26: Along-channel 1% JPM water levels for the NC SLRIS scenarios. Top) 1% JPM levels with tides and error term. Bottom) 1% JPM levels with surge-only.

The lower plot (JPM, no tides, no error) indicates that, even without the tides, the flood water levels do not behave in a strict “bathtub” sense.

In response to this concern, RENCI has scrutinized the model output and determined that the model responses are well within expectations, given the extent of geomorphological changes to the underlying scenario topography and bathymetry, which determines the ADCIRC grid elevations. Additionally, the unexpected behavior of SWEL levels can be explained by considering the tidal response to a river channel that 1) strongly converges in terms of cross-channel width and depth converging and 2) that has a substantial intertidal storage area that **also** increases as sea level increases. This storage volume (defined as the volume of water contained between the channel topo/bathy and the MHW and MLW water surfaces) generally increases as sea level increases. However, the storage volume may change due to morphological considerations that are themselves a complicated response of increased sea levels, modified tidal regime, etc. Of course, in ADCIRC, the topo/bathy is static, meaning that for a given scenario and tidal regime, the effects of the sea level increase can be reasonably understood.

A purely linear, “bathtub” perspective motivates the expectation that SWEL, tidal amplitudes, and tidal datums increase relatively monotonically with the imposed static sea level increment. This would be largely correct if geometric considerations of the river could be ignored and (more importantly) if there were no imposed geomorphological changes on the river basin. In the limit of a channel with vertical walls (i.e., no floodplain), then the bathtub expectation is essentially correct. For a detailed analysis of idealized channel response to tidal forcing under sea level increases, see Friedrichs, Aubrey, and Speer (1990).

In rivers with complex geometries, the tidal water level response a sequence of sea level increases depends critically on how the intertidal storage volume increases. As this volume increases, tidal amplitudes may **decrease** as the incoming tidal wave is reflected less. The consequence of decreasing reflection is that the progressive character of the wave increases, in response to increased conveyance upstream to fill the increased volume. If the volume increase is small, then the increased mass flux needed to fill that volume is also relatively small and tidal amplitudes will decrease a small amount. However, if the volume change is large, then the tide propagation characteristics can change substantially.

3.1. Idealized Model Experiments

To illustrate this dependency, and in addition to the engineering and coastal oceanographic literature, we have conducted a sequence of tidal simulations with idealized rivers. The basic Cape Fear geometric characteristics are used to define the along-channel dependence on the cross-channel width and depth profiles. In particular, cross-channel depth profiles were taken upstream in the NC SLRIS Baseline and 100cm grids and used to define the topo/bathy in the idealized grids. The mouth of the Cape Fear River is about 1 km wide, but the river width expands substantially immediately upstream. This is indicated in the grid figures below as the widening of the river between 0 and 3 km.

The idealized river is 70 km long with a constriction in channel and bank width at about 40 km. This places “Wilmington” at about 45 km upstream. This baseline geometry is shown in Figure 27.

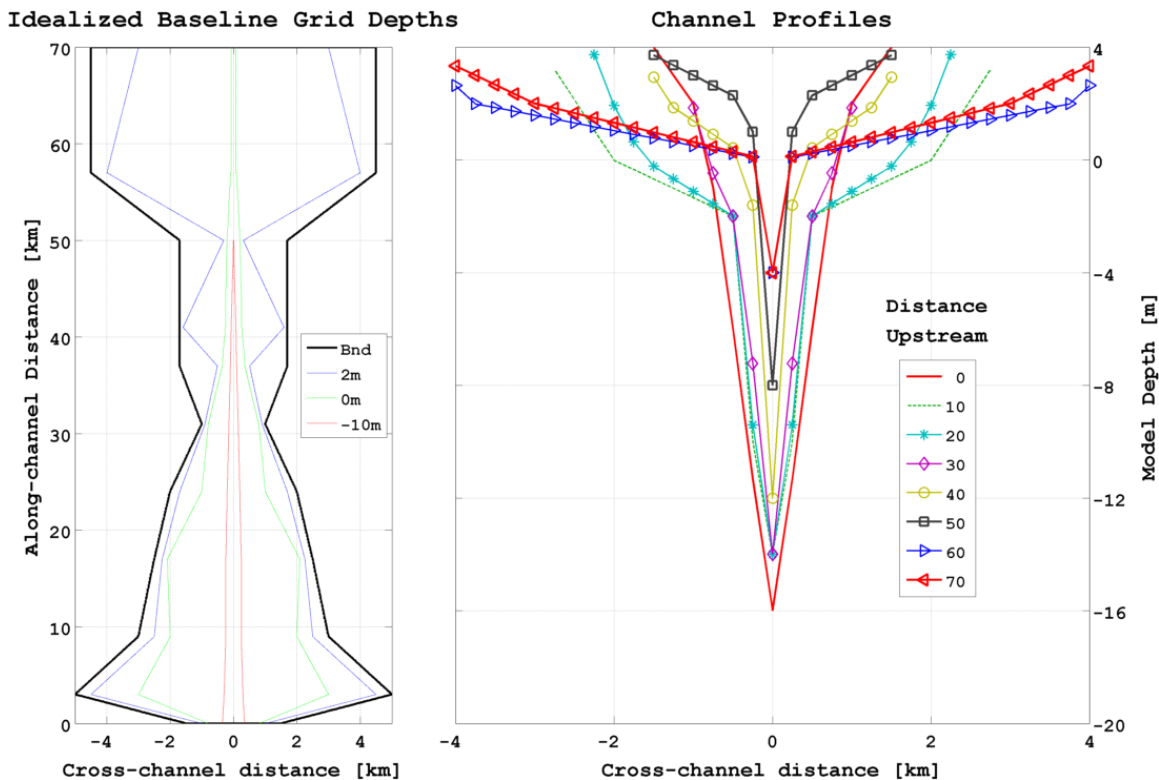


Figure 27: Idealized baseline grid geometry. Left) Plan view of grid, with 2, 0, and -10 meter grid elevation contours. The thick black line is the grid’s exterior boundary. Right) Cross-channel depths at 10 km intervals along-channel. The profile at 50 km (black squares) is the narrowest part of the channel.

To represent the end-member SLR scenario of a substantially altered storage volume in the upper (north of Wilmington) Cape Fear River, the baseline grid depth profiles are modified to broaden AND deepen the storage upstream of about 50 km. This grid is shown in Figure 28. In addition to a 1-meter increase in mean sea level, the upper basin is deepened to increase the volume. Each configuration includes a deep central channel with variable-width along-channel floodplain banks.

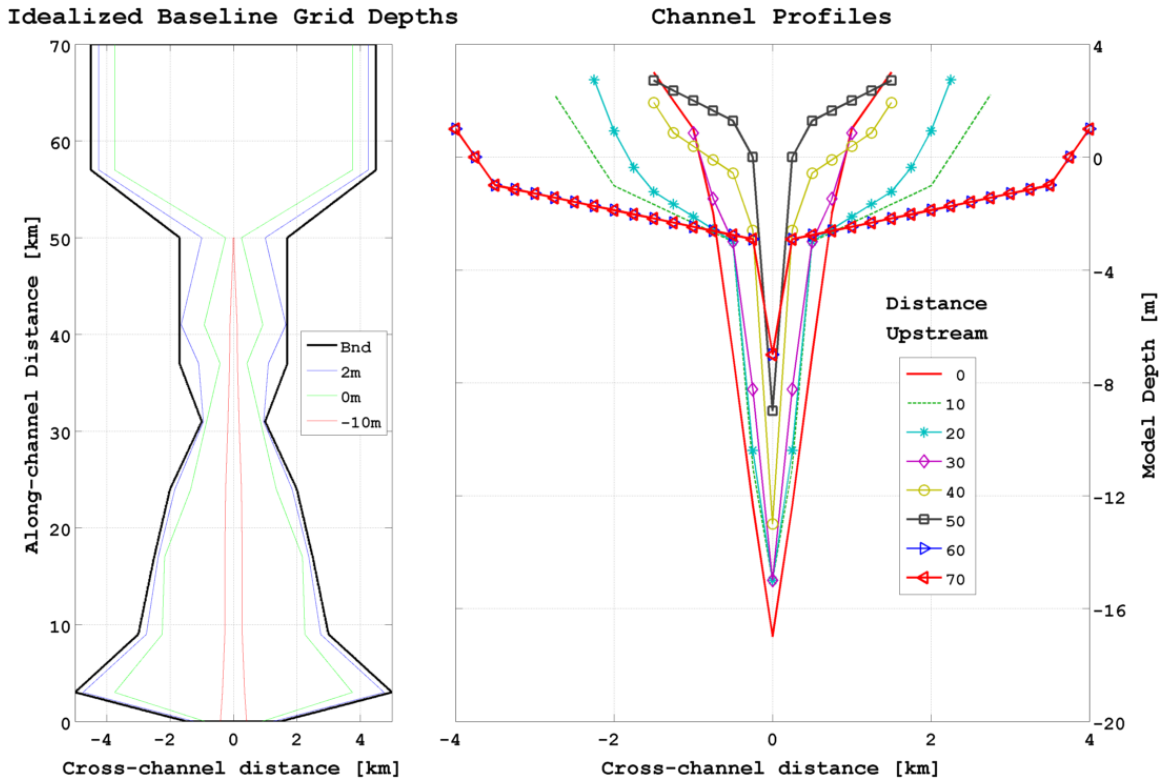


Figure 28: Idealized grid geometry with increased storage capacity on the upper basin. Left) Plan view of grid, with 2, 0, and -10 meter grid elevation contours. The thick black line is the grid's exterior boundary. Right) Cross-channel depths at 10 km intervals along-channel. The profile at 50 km (black squares) is the narrowest part of the channel.

Three simulations were conducted to shed light on the tidal dynamics in channels with varying tidal storage volumes in an upper basin:

1. Baseline geometry (Figure 27) with no sea level increase.
2. Baseline geometry with a 1-meter sea level increase - This is the grid in Figure 27 with a datum offset of +1 meter.
3. Deeper upper basin geometry with a 1-meter sea level increase (Figure 28).

Simulation parameters include:

1. 10 days long with a 2 day rampup.
2. Harmonic analysis over days 6-10.
3. Elevation boundary condition of an M_2 tide with 1-meter amplitude and 0 phase.
4. No rotation.
5. Constant Manning's N.

3.2. Idealized Model Results

The nature of the tides in these idealized scenarios is investigated by looking at the primary tide elevation response in the along-channel direction. Figure 29 shows the along-channel M_2 elevation amplitude (black) and phase (red) for the three scenarios. For all scenarios, the tidal amplitude drops slightly due to the expansion of the river width immediately upstream of the open boundary. Case 1 and 2 (both on the baseline grid geometry) amplify slightly from the minimum amplitude at 10 km. However, the case1 amplitude increases relative to the boundary condition by about 10%. The distance at which the amplitudes begin to drop substantially is most upstream in case one, at about 55 km. Case 3 (deeper upper basin AND 1 m SLR) exhibits this character at about 45 km, which is in the vicinity of “Wilmington” in the idealized geometry.

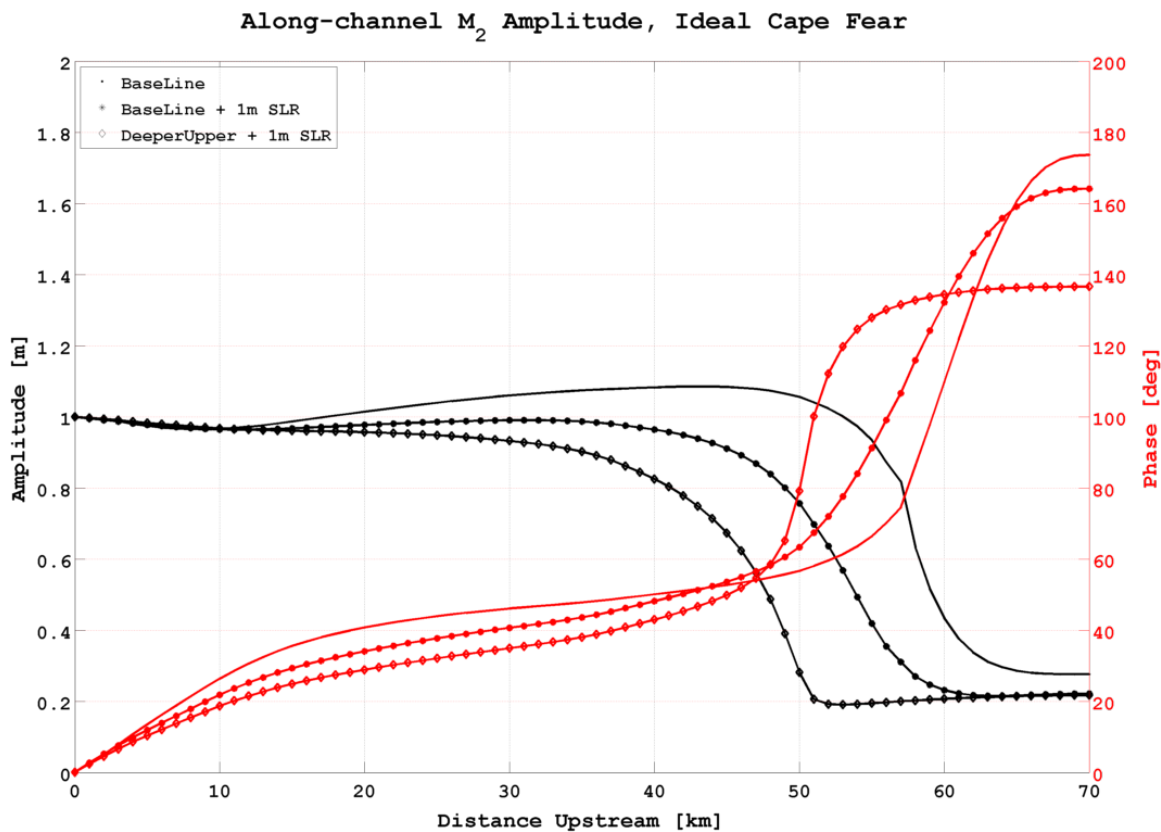


Figure 29: Along-channel M_2 Elevation amplitude and phase for the 3 idealized cases.

In the case 1 scenario, the tide amplifies due to the convergent nature of the channel. This amplification decreases as the average water depth increases AND the river widths widen (less convergent). The M_2 elevation phase increases upstream (later arrivals) and undergoes substantial lags upstream of about 50 km. The phases are all about 60 deg in the idealized Wilmington area, but as the water deepens and storage volume increases, the tide arrives earlier in the upper basin area.

Next, we consider the along-channel tidal velocity component. This is shown in Figure 30. The velocity amplitudes are all relatively smaller and relatively the same in the lower river area. However, just downstream of the channel constriction, the velocity increases due to the converging channel. For the baseline grid (case 1 and 2), the upstream velocity peaks at about 1.35 m/s, with the maximum occurring more upstream in case 1. The abrupt changes in speed are due to the transition of the channel depths. In case 3 (deeper upper basin with 1 m SL increase), the peak velocity exceeds that at the open boundary and occurs more downstream relative to the baseline grid cases. The more rapid drop in speed is due to the rapidly increasing storage area.

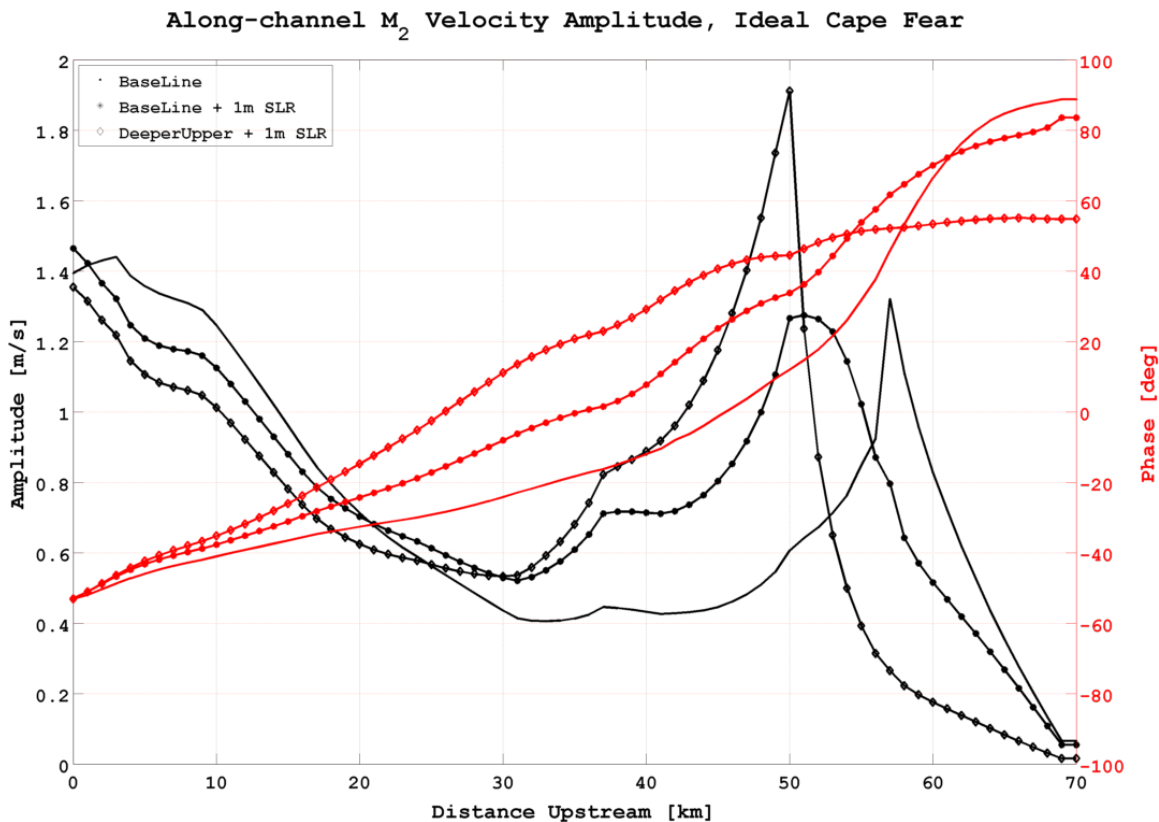


Figure 30: Along-channel M_2 velocity amplitude and phase for the 3 idealized cases.

While the elevation and velocity amplitude and phase are illustrative of the impacts of increased storage volumes in the upper river basin, they themselves do not reflect the transition of the incoming tide wave from more standing (case 1) to more progressive (case 3). Recall that for a standing wave, the water level and velocity are out of phase by 90 degrees, and for a purely progressive wave the elevation and velocity are exactly in phase. So it is the phase difference between elevation and velocity that is most relevant to the nature of the tidal wave. Figure 31 shows this difference for the 3 idealized cases. In the baseline case 1, the tide becomes more standing in character (relative to the open boundary phase difference) and shifts toward a mixture of standing and progressive upstream of the narrowest part of the channel. The smallest phase difference is about 30 degrees. The case 2 (baseline + 1 m) phase

difference is relatively similar to case 1, with an “earlier” minimum near 50 km and less of a difference in the lower channel area. The minimum is still about 30 degrees.

However, in case 3, the character is substantially different from the baseline cases. The partitioning of the wave between standing and progressive almost immediately moves towards progressive, with the wave becoming almost entirely progressive in the “Wilmington” area, and a “rapid” transition toward almost fully standing in the deeper upper basin. Of course, at the head of the channel in all cases, there is significant reflection and hence an almost entirely standing wave phase difference near 90 deg.

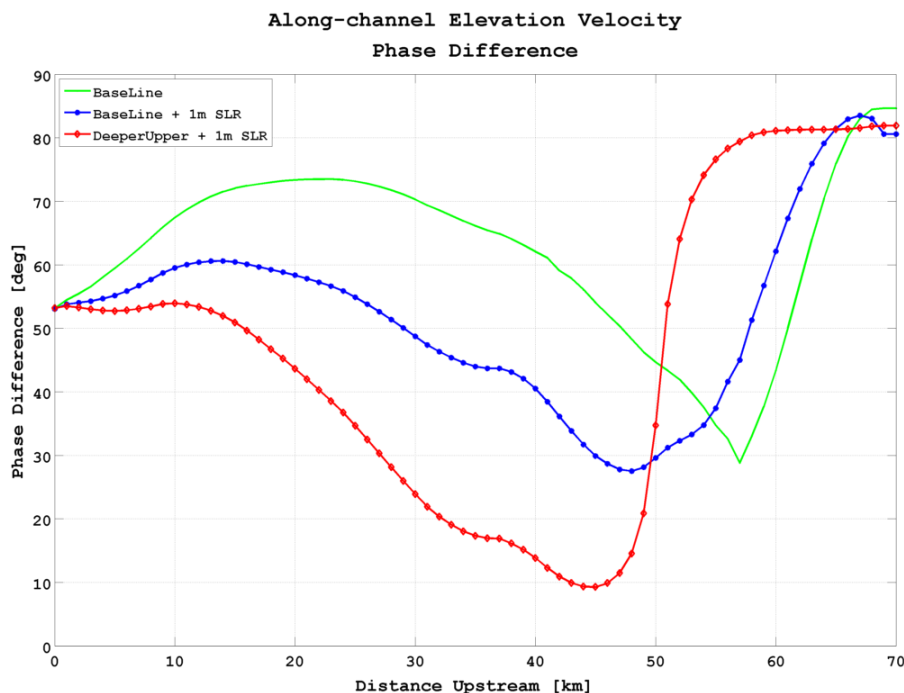


Figure 31: Along-channel phase difference between elevation and the along-channel velocity for the M₂ tide

3.3. Connection of Idealized Results to NC-SLRIS

In the NC-SLRIS project, a sequence of SLR amounts is added to the Baseline grid or a grid to which some level of geomorphological adjustments have been imposed. The 100cm end-member scenario has a substantially increased storage volume, as compared to just adding sea level increases to the baseline geometry. This is illustrated in Figure 32, which shows the change in storage volume with increasing SL for the 6 project scenarios. The red line is the tidal storage volume (in cubic km) below the scenario’s MSL, using the grid for that scenario. The green line is the volume below mean high water. The volume increases are large, with a 5-fold increase in the storage volume below MSL. For comparison, the blue line is the volume below MSL for each scenario but computed relative to the baseline grid. Note a slightly exponential

increase as sea level increases, an expected feature of volume increase with increasing water levels in basins with gently sloping sidewalls.

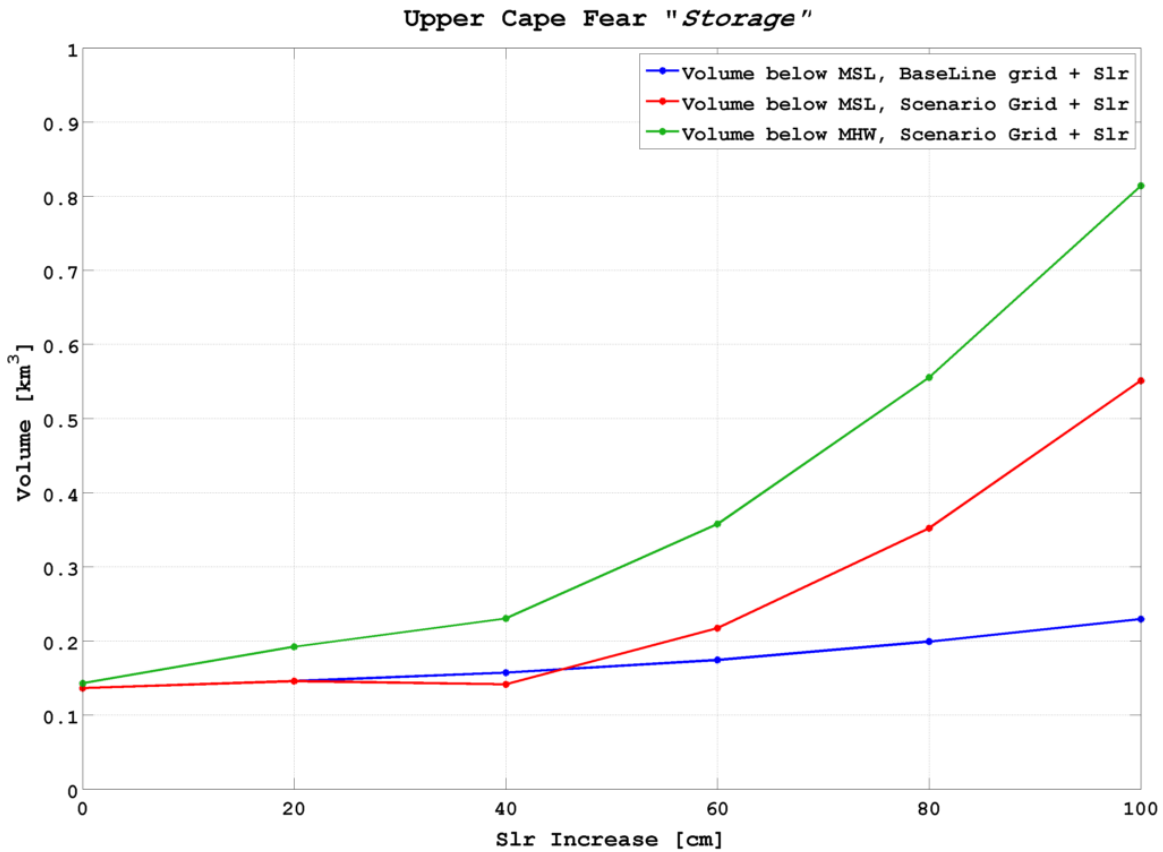


Figure 32: Tidal storage volumes in the Cape Fear River, upstream of Clarks ad Eagle Islands, for the project scenarios. The blue line indicates storage computed with the sea level increase but with the baseline grid topography/bathymetry.

The impact of tidal storage changes (increases) on the M_2 tide propagating up the Cape Fear River is shown in Figure 33. The general characteristics are very similar to the idealized results discussed above. For the scenarios that are close to the Baseline (00 cm, 20 cm, 40 cm), in terms of upper basin storage volume, there is a relatively small change in the tidal elevation, although there is a slight amplitude increase due to slightly deeper water and little geometric change upstream of Wilmington. However, as the storage volume increases (red line, Figure 32) upstream of Wilmington, tidal amplitudes drop and the phase is lagged. The amplitude difference between the scenario end-members is about 60 cm.

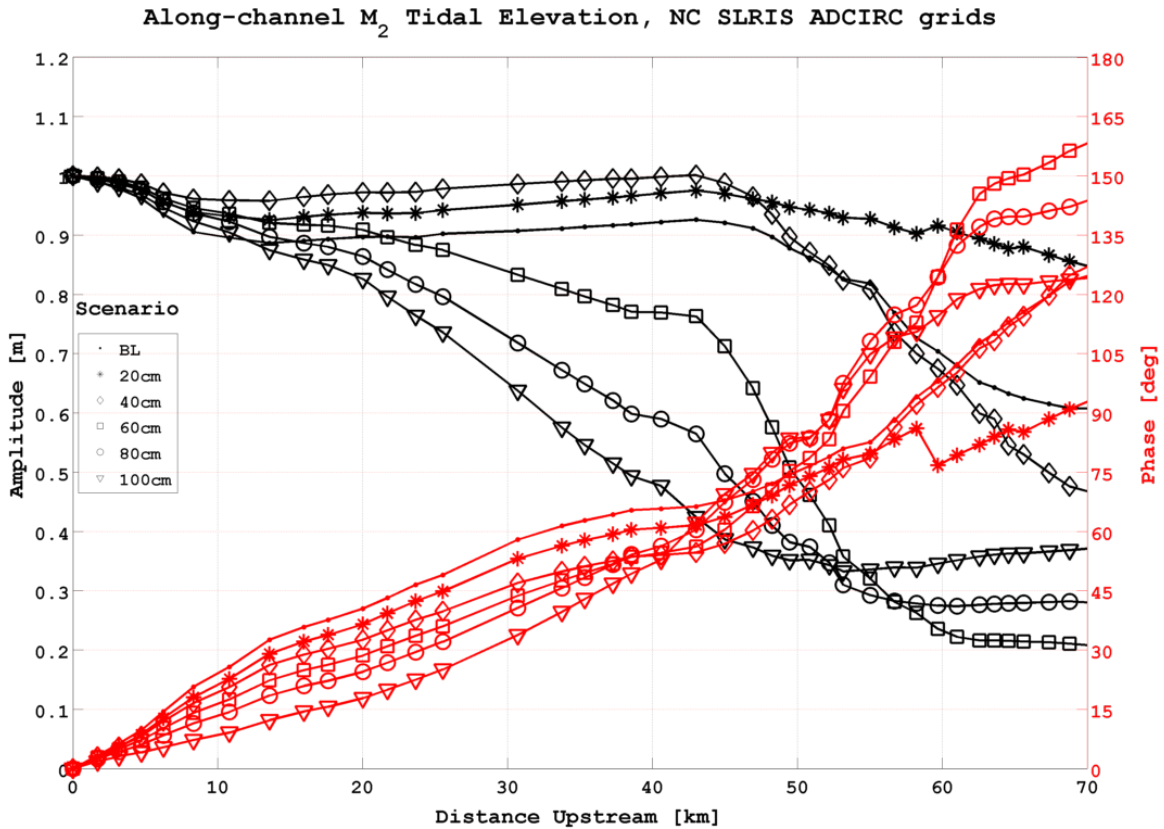


Figure 33: Along-channel M₂ tidal elevation amplitude and phase in the Cape Fear River.

The phase angle between the elevation and velocity, indicative of the mixture between standing (toward 90 deg) and progressive (toward 0 deg), is shown in Figure 34 for the Baseline and 100 cm scenarios. Due to the realistic and more complex river/channel characteristics, the velocity exhibits much more variability than in the idealized cases. Nonetheless, the phase angle for the 100 cm scenario is substantially more toward 0 (progressive, in phase) in the lower part of the river than in the Baseline scenario. The baseline scenario is generally an approximate balance between standing and progressive and overall does not change as much as in the 100 cm scenario.

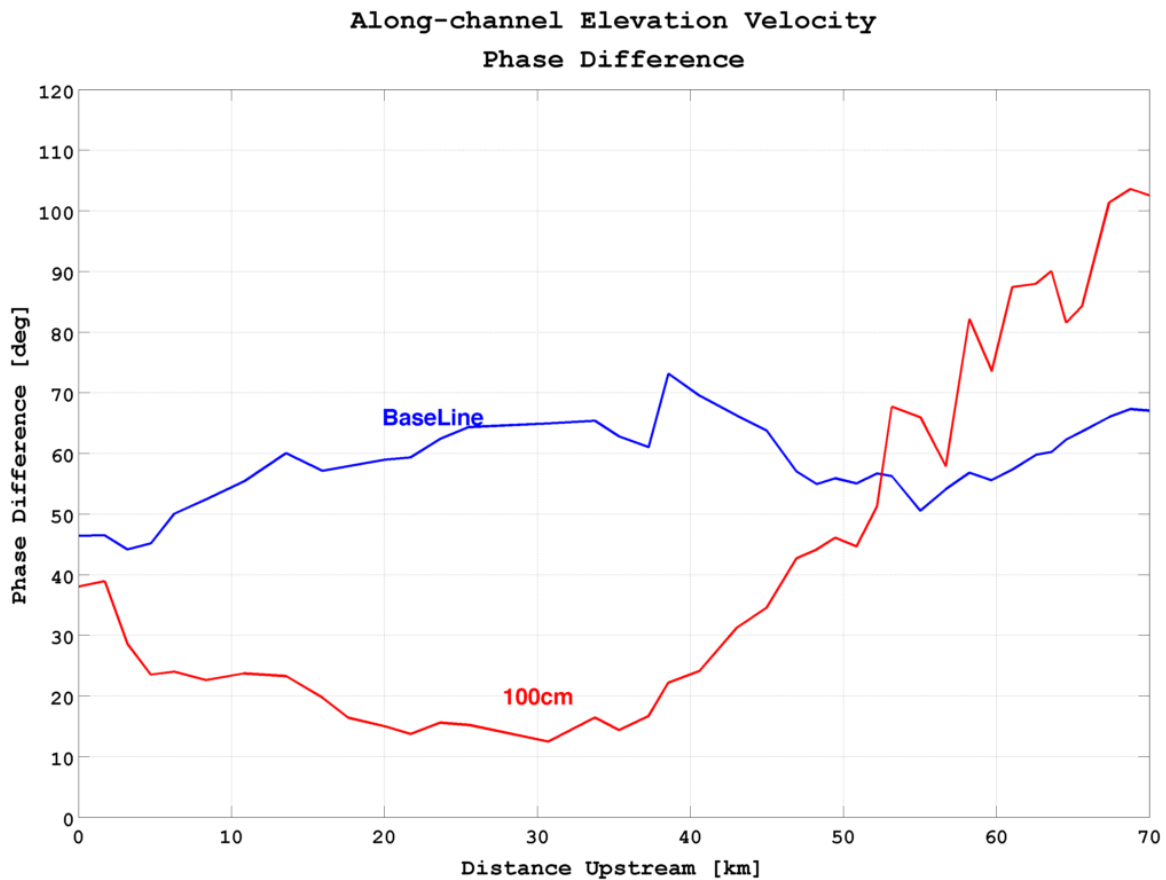


Figure 34: Along-channel phase difference between M2 tidal elevation and velocity. Only the Baseline (blue) and 100cm (red) scenarios are shown.

The storage volume increases also affect storm surges in a similar way, although the diagnostic quantities like phase angle not meaningful in this context. To illustrate the impact of the storage volume on the simulated water levels, the along-channel maximum water level for the 1993 extratropical storm (Storm of the Century) is shown in **Error! Reference source not found**. Figure 35. The water level response in the Baseline scenario is that the surge is amplified up the channel to the Wilmington area, upstream of which there is a reduction of water level. This characteristic is generally the case for the first 3 scenarios.

However, as the storage volume increases, two things happen. 1) Water volume flows past the Wilmington area, filling in the storage increase, and raising water levels in the upper basin. 2) This volume of water is no longer stored in the lower part of the river, as indicated by the generally flat water level in the 80 and 100 cm scenarios. In other words, the water that would otherwise fill in the lower river floodplain is, in later scenarios, being driven into the larger basins upstream of Wilmington.

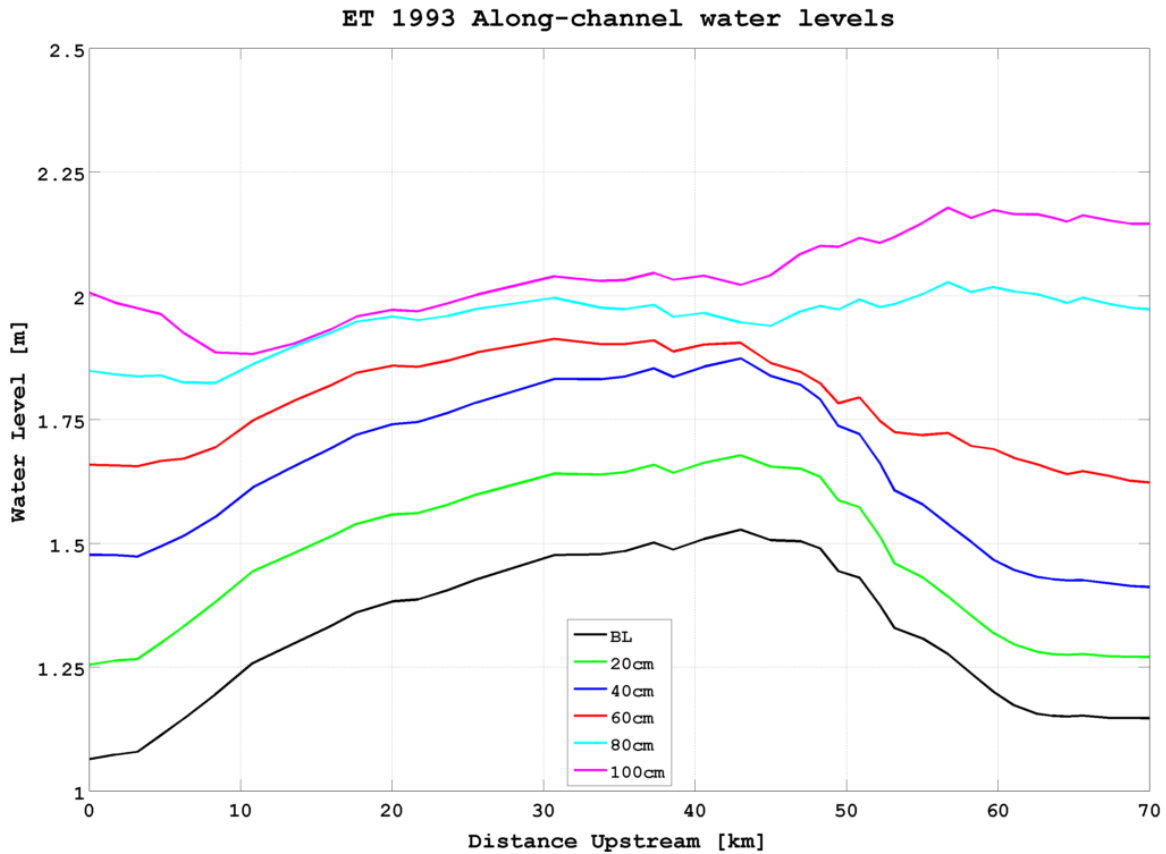


Figure 35: Along-channel water level for the extra-tropical storm 1993.

3.4. Idealized Results Conclusion

The implications of this decreased tidal amplitude with increasing storage volume are that the tidal contributions to the statistical flood levels will be less in “later” scenarios, in which the larger storage volumes occur. In these idealized experiments the tidal amplitude at “Wilmington” decreases from about 1.1m to 0.6 m, implying that if the non-tidal SWEL levels increase by 1 meter between the NC SLRIS end-members, then it can be expected that the total combined SWEL + tides will not increase at the same level as the sea level increase. It seems unlikely that effects of channel dredging can have an appreciable impact on the tidal and surge dynamics in the Cape Fear River system, although local (to the gauged location) effects are probable.

4. REFERENCES

- Blanton, B.O., 2008, North Carolina Coastal Flood Analysis System: Computational System. *Technical Report TR-08-04*, RENCI, North Carolina, September 2008.
- Egbert, G. D., Bennett, A., and Foreman, M. G. G. (1994). TOPEX/Poseidon tides estimated using a global inverse model. *J. Geophys. Res.*, 99:24821–24852.
- Friedrichs, C. T., D. G. Aubrey, and P. E. Speer (1990), Impacts of relative sea-level rise on evolution of shallow estuaries, in *Residual Currents and Long-Term Transport, Coastal Estuarine Stud.*, vol. 38, edited by R. T. Cheng; 122, AGU, Washington, D. C., doi:10.1029/CE038p0105.
- Scheffner, N.W., L.E. Borgman, and D.J. Mark, 1996, Empirical simulation technique based storm surge frequency analyses, *Journal of Waterway, Port, Coastal and Ocean*, Vol. 122, No. 2, 93-101.
- Scheffner, N.W., Clausner, J.E., Militello, A, Borgman, L.E., Edge, B.L., and Grace, P.E., 1999. Use and application of the empirical simulation technique: User's Guide. *Technical Report CHL-99-21*. U.S. Army Engineer Research and Development Center, Coastal and Hydraulics Laboratory, Vicksburg, MS, 194 p.
- Vickery, P.J., D. Wadhera, M.D. Powell and Y. Chen, 2009, A Hurricane Boundary Layer and Wind Field Model for Use in Engineering Applications, *Journal of Applied Meteorology and Climatology*, Vol .48, 381-405, DOI: 10.1175/2008JAMC1841.1.
- Vickery, P.J. and B.O. Blanton, 2008, North Carolina Coastal Flood Analysis System: Hurricane Parameter Development. *Technical Report TR-08-06*, RENCI, North Carolina, September 2008.
- Westerink, J.J., R.A. Luettich, Jr., J.C. Feyen, J.H. Atkinson, C. Dawson, M.D. Powell, J.P. Dunion, H.J. Roberts, E.J. Kubatko, H. Pourtaheri, 2008. "A Basin- to Channel- Scale Unstructured Grid Hurricane Storm Surge Model as Implemented for Southern Louisiana", *Monthly Weather Review*, 136:833-864, DOI: 10.1175/2007MWR1946.1.